ECLÉTICA QUÍMICA

Original Article

Eclet. Quim. 49 | e-1526, 2024

https://doi.org/10.26850/1678-4618.eq.v49.2024.e1526

Evaluation of the effectiveness of new mixed ligand complexes against the vector of Dengue fever *Aedes aegypti* (Diptera; Culicidae)

Nedhal Abdulmawla **Al–Selwi**[1], Abbas Mohamed **Al–Azab**[1], Yasmin Mosa'd Saeed **Jamil**[1+], Fathi Mohamed **Al–Azab**[1], Anwar Mohamed **Al–Ryami**[1]

Abstract

Chloroquine phosphate with ibuprofen and sulphamethoxazole were used as mixed ligands with Ni(II), Co(II), Cu(II), and Zn(II) to prepare new transition metal complexes. Metal analysis, IR, and X-ray diffraction (XRD) spectrum analyzes were used to describe them, with some modifications to the World Health Organization (WHO) standard susceptibility test under laboratory conditions. The biological effects of ligands and new complexes against *Aedes aegypti* mosquito larvae were evaluated at various concentrations. To assess larvicidal efficacy, late third or early fourth instar larvae were exposed to multiple concentrations of the examined compounds, ranging from 50 to 1000 ppm. Cu(II) complexes revealed significant high activity (LC_{50} = 100 ppm against *Ae. Aegypti* was compared with the rest of the metal complexes. On the other hand, the Co(II) complex showed no activity against *Ae. aegypti*. These mixed ligand complexes seemed to be an alternative method for manufactured insecticides to control larvae of this medically important mosquito vector *Ae. aegypti*. Further research on other metal complex compounds responsible for larvicidal efficacy will be required.

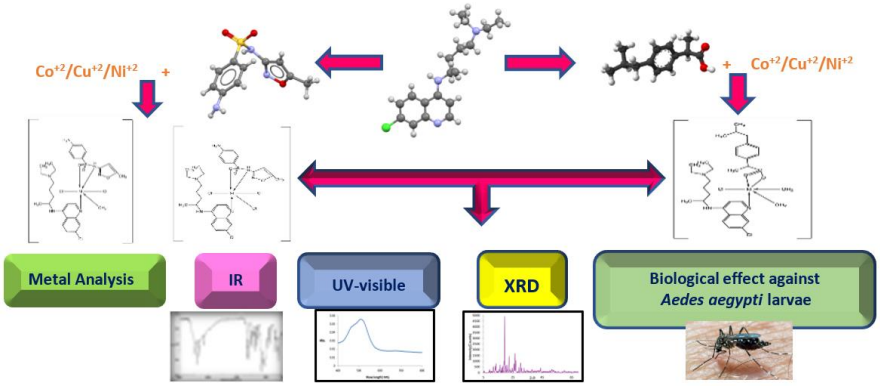

Article History

Received October 20, 2023
Accepted May 10, 2024
Published August 21, 2024

Keywords

1. complex;
2. mixed ligands;
3. XRD;
4. *Aedes aegypti*;
5. dengue fever.

Section Editor

Rogéria Rocha Gonçalves

Highlights

- Chloroquine phosphate was used with ibuprofen and sulphamethoxazole as mixed ligands.
- The mixed ligands were complexed with Ni(II), Co(II), Cu(II), and Zn(II).
- The biological effects against *Aedes aegypti* mosquito larvae were evaluated.
- The Cu(II) complexes revealed higher activity against *Aedes aegypti* than others.

[1]Sana'a University, Faculty of Science, Sana'a, Yemen. **+Corresponding author:** Yasmin Mosa'd Saeed Jamil, **Phone:** +967771952842, **Email address:** y.jamil@su.edu.ye

1. Introduction

Mosquitoes belong to the order Diptera presented worldwide in most ecosystems. They are widely distributed around the world and can transmit viral, protozoal, and helminth diseases to human beings, such as dengue fever, chikungunya, West Nile virus, yellow fever, Rift Valley fever, malaria and elephantiasis in almost all tropical and subtropical countries, as well as many other parts of the world (Chew *et al.*, 2019; Netoi *et al.*, 2018).

Aedes aegypti Linnaeus was described in 1762 (Bar *et al.*, 2013). In most of the world, it is the primary vector for dengue (WHO, 2009), yellow fever (Al–Azab *et al.*, 2020), zika (Fauci and Morens, 2016; Marcondes and Ximenes, 2015; Schrauf *et al.*, 2020), chikungunya (Charrel *et al.*, 2014). Due to its strong ties to people, *Aedes aegypti* is significant. Unlike other animals, females attack people. They lay their eggs near human habitations in man-made containers, typically breeding grounds that are not completely covered with many organic resources for larval nutrition. *Aedes aegypti* has become more adapted to urban surroundings all over the world due to unchecked urbanization, rising temperatures, and a lack of long–term vector control measures (David *et al.*, 2021; Leandro *et al.*, 2023; Maciel-de-Freitas *et al.*, 2007; Scott *et al.*, 1993).

In some tropical and subtropical countries in the past 30 years, dengue fever outbreaks have grown ten times (Simmons and Farrar, 2009; WHO, 2009). The dengue virus has infected more than 3 billion people around the world and is responsible for more than 20,000 deaths annually. A total of 128 countries are in danger (Bhatt *et al.*, 2013; Rajaganesh *et al.*, 2016; Suresh *et al.*, 2015).

Dengue fever (DF) is a common local endemic infectious disease that mainly affects underdeveloped areas of Yemen and has high mortality and severity rates. This prevalence and geographic expansion of epidemic dengue have hurt Yemen, and the number of reported cases has increased in lockstep with the nation's social upheaval and civil war (Alyousefi *et al.*, 2016; Gutu *et al.*, 2021). Since 2000, there have been regular outbreaks of DF in Yemen, where it was initially identified in the Shabwah governorate in 1994. Aden and Taiz (2010; 2020), Hadramout and Mulalla (2005), and Al-Hudeidah Governorate, Yemen (1994, 2000, 2004, and 2005), outbreaks have been detected in Shabwah Governorate in 2001, 2002, 2005, 2018, 2019, and 2020 (unpublished reports) (Bin Ghouth *et al.*, 2012; Gutu *et al.*, 2021).

Chloroquine (CQ), an antimalarial drug, was first developed in the 1930s. It is produced by a convergent synthesis in which the aliphatic components (novaldiamine, 2–amino–5–dimethylaminopentane) and the quinoline parts (4,7–dichloroquinoline) are combined in the final stage of aromatic nucleophilic displacement. Although affordable and widely available, chloroquine is no longer highly effective against *P. falciparum*, the most lethal strain of the malaria parasite, due to drug resistance (Kucharski *et al.*, 2022; V. Singh, 2019).

The bacteriostatic agent sulfamethoxazole (SMX) is an antibiotic ften used for the treatment of many infections. Due to its common use, humans and animals can develop active and unmetabolized metabolites that have a variety of biological effects (Jasim *et al.*, 2022). In both human and veterinary medicine, is a frequently prescribed antibiotic that is also used as a sulfonamide in aquatic and terrestrial environments. In a European assessment of medicine and personal hygiene items, it was also included in the top 10 lists of essential drugs (Rauseo *et al.*, 2019).

One non–steroidal anti-inflammatory medicine (NSAID) that has therapeutic effects is Ibuprofen, which inhibits both the COX1 and COX2 isoforms of the cyclooxygenase enzyme. The production of prostaglandins, which are endogenous mediators implicated in the start of pain, inflammation, and fever, is catalyzed by this enzyme (Singh, 2019; Kucharski *et al.*, 2022).

Metals have always attracted researchers in modern medicine because of their significant involvement in physiological and pathological processes, and their antibacterial, antifungal, anti-inflammatory, and antimalarial capabilities. In many fields as molecular biology, photochemistry, bioinorganic chemistry, medicine, and chemistry, mixed ligand–metal complexes are essential (Muthuppalani *et al.*, 2022; A. Singh *et al.*, 2020). The biological features of these compounds and their inherent chemical value as multidentate ligands have been influenced by specific central metals, particularly Cu(II), Zn(II), Fe(III), Ni(II), Co(II), etc. This has led to a substantial improvement in the research on their coordination behavior (Kumar *et al.*, 2021). One of the main goals of modern inorganic coordination chemists and pharmaceutical research is to find and produce more effective pharmaceuticals to treat ailments. This has led to several investigations of drug–metal complexes (Adediji *et al.*, 2018), and researchers are exploring the therapeutic potential of metal-based antimalarial agents, especially since the discovery of ferroquine, once the most potent organometallic antimalarial drug (Biot *et al.*, 2011).

In this work, the potential larvicidal activities of these compounds are evaluated together with the production and characterization of complexes from chloroquine phosphate, ibuprofen and sulphamethoxazole with transition–metal ions.

2. Experimental

2.1. Materials

High–purity chemicals were used by many companies. Chloroquine phosphate, ibuprofen (Ibu), and sulphamethoxazole were obtained from Shaphaco Pharmaceutical Company. Other chemicals, solvents, indicators, and metal (II) chlorides (nickel chloride hexahydrate, cobalt chloride hexahydrate, copper chloride dehydrate, and zinc chloride hexahydrate) from BDH were used without further purification.

2.2. Preparation of metal complexes

In general, aqueous solutions of hydrated metal chlorides, chloroquine phosphate, and (10% ammonia solution of ibuprofen or 10% potassium hydroxide solution of sulphamethoxazole) in 1:1:1 mole ratio are prepared. The combination of the corresponding three solutions was refluxed on a hot plate for 3 h at 60–80 °C with constant stirring to obtain colored precipitates. Filters were used to obtain the solid precipitates, then carefully cleaned in hot water and dried by air (Muthuppalani *et al.*, 2022).

2.3. Physical Measurements

The Central Laboratory of the Faculty of Science of Cairo University, Giza, Egypt, used a Vario EL Fab. CHNS Nr to conduct the C, H, N, and S element analysis. At the Global Pharmaceutical Company, the metal content was evaluated using an atomic absorption spectrophotometer with standard solutions of metal chlorides used for calibration. A definite weight of the solid complexes was digested with 10 mL of concentrated HNO_3. This was repeated several times until all the organic matter was completely decomposed. The reaction mixture was evaporated just to dryness. After being cooled, the residue complex was dissolved in distilled water (Bader, 2011). At the Global

Pharmaceutical Company, a Sartorius conductivity meter model pp20 was used to measure the molar conductance of 10^{-3} mol L^{-1} solutions of metal complexes in 10% DMSO (dimethylsulfoxide) solvent. For the freshly produced solutions, all measurements were made at room temperature. At Sana'a University, the infrared spectra of the complexes were measured using an FT/IR–140 spectrophotometer with a KBr disc (4000–400 cm^{-1}) from Jasco, Japan.

A magnetic susceptibility balance from the Johnson–Metthey and Sherwood model was used to measure magnetic susceptibilities using Gouy's approach (Szafran *et al.*, 1991). The effective magnetic moment (μ_{eff}) values were obtained using the Eqs. 1–3).

$$X_g = \frac{C_{Bal} L (R - R_0)}{10^9 M} \quad (1)$$

where R_o=Reading of empty tube, L=Sample length (cm), M=Sample mass (g), R=Reading for the tube with sample, C_{Bal}=balance calibration constant=2.086

$$X_M = X_g . MWt \quad (2)$$

The values of X_M as calculated from Eq. 2 are corrected for the diamagnetism of the ligands using Pascal's constants, then used in Curie's Eq. 3.

$$\mu_{eff} = 2.84\sqrt{X_M . \ T} \quad (3)$$

where T = t (°C) + 273

All melting points for the compounds are given in degrees Celsius and are measured in glass capillary tubes. Silver nitrate was used to determine chloride using a gravimetric method (Jamil *et al.*, 2022a). The weight loss approach allowed us to gravimetrically calculate the number of coordinated and uncoordinated water molecules (Refat *et al.*, 2014). TLC was carried out on Silica Gel GF_{254} plates (mn–kieselgel G., 0.2 mm thickness) with acetone solution as mobile eluent at room temperature (25 °C), plates were scanned using an ultraviolet 254 nm lamp. XRD patterns were obtained using an XD–2 powder X-ray diffractometer (Shimadzu ED–720) at a voltage of 35 kV and a current of mA using CuK(α) radiation in the range of $5° < 2\theta < 70°$ at 1° min^{-1} scanning rate and a wavelength 1.54056 Å, in Yemen Geological Survey and Mineral Resources Board.

2.4. Crystallinity and particle size from XRD

The percentage of crystallinity, XC (%) was calculated based on the integrated peak areas of the principal peaks (Jamil *et al.*, 2023a). The crystallinity of the complexes is calculated relative to the crystallinity of the ligands as a ratio (Eq. 4):

$$XC\ (\%) = \left[\frac{(A_{ligand})}{(A_{complex})}\right] \times 100 \quad (4)$$

where $A_{complex}$ and A_{ligand} are the areas under the principal peaks of the complex and ligand sample, respectively.

XRD was also used to determine the average particle size (D), which was estimated by the Scherrer equation (Eq. 5) (Patterson, 1939; Saeed *et al.*, 2015).

$$D = \frac{K\lambda}{\beta \cos\theta} \quad (5)$$

where K is Scherrer constant and equals 0.94, λ is the X-ray wavelength of Cu–Kα radiations (1.5405 Å), β is the full width at half maximum (FWHM) and θ is the Bragg diffraction angle in degrees.

2.5. Source of mosquito strain and rearing

2.5.1. Insects: mosquitoes

Aedes aegypti (Diptera; Culicidae) were obtained from untreated sites using insecticides from Sana'a city.

2.5.2. Mosquito strain rearing

The larvae of *Ae. aegypti* were reared under laboratory conditions of medical entomology, Department of Biological Sciences, Faculty of Science – Sana'a University for over several generations using fish food diet medium, larvae from culture.

2.5.3. Bioassay of mixed ligand complexes against *Ae. aegypti* (L.)

The larvicidal bioassay followed the WHO (2008) standard protocols with some modifications. Individual ligands and metal complexes were dissolved in 3% DMSO and the results were recorded 24 h later.

3. Results and discussion

After being washed with hot water, the Ni(II), Co(II), Cu(II), and Zn(II) complexes produced with the ligands were collected. Because of this, the complexes on their thin–layer chromatography displayed single spots with acceptable Rf values, indicating their pure condition. Insoluble in water, ethanol, methanol, acetone, $CHCl_3$, 0.1 mol/L NaOH, and dimethylformamide (DMF), all complexes were pigmented and stable in the presence of air but were all soluble in DMSO 10% and 0.1 mol/L HCl. The new complexes have melting points higher than those of the pure ligands. The melting points of Ni(II), Co(II) and Cu(II) complexes with the complex (CQ)(Ibu) and [Zn(CQ)(SMX)Cl_3] were (> 350 °C). The melting temperatures of the other materials ranged from 204 to 254 °C. The complexes of Ni(II), Co(II), Cu(II) and Zn(II) exhibited molar conductivity values between 7 and 15 Ω^{-1} mol^{-1} cm^2, indicating the non–electrolytic nature of these complexes (Jamil *et al.*, 2022b). Some physical properties and analytical data of these complexes are listed in Tables 1 and 2.

Table 1. Some physical properties of the complexes.

Compound	Color (Yield%)	M.P. (°C)	Λm (Ω^{-1} cm^2 mol^{-1})	μeff (B.M.)	F.Wt (g/mol)	TLC	
						No. of Spots	R_f*
[Ni(CQ)(Ibu)$(H_2O)_2$Cl]	Light yellow (21)	>350	9	3.09	655.343	One	0.81
[Co(CQ)(Ibu)$(H_2O)_2$Cl]	Dark purple (26)	>350	7	4.75	655.583	One	0.71
[Cu(CQ)(Ibu)$(H_2O)_2$Cl]	Light green (20)	>350	8	1.68	660.199	One	0.54
[Zn (CQ)(Ibu)$(H_2O)_2$Cl]	White (22)	240	7	–	662.033	One	0.67
[Ni (CQ)(SMX)$(H_2O)Cl_2$]	Light green (36)	204	15	3.01	720.791	One	0.85
[Co (CQ)(SMX)$(H_2O)Cl_2$]	Pink (22)	254	14	5.05	721.001	One	0.74
[Cu (CQ)(SMX)Cl_3]	Sky blue (25)	220	12	1.73	743.055	One	0.49
[Zn (CQ)(SMX)Cl_3]	White (28)	>350	14	–	744.889	One	0.61

Note: *R_f = retention factor in Thin Layer Chromatography

Table 2. Elemental analysis of the complexes.

Complex (Molecular formula)	Element Analysis, Found (Calculated)%					
	C	H	N	S	M	Cl
[Ni(CQ)(Ibu)$(H_2O)_2$Cl]	56.82	7.21	6.42	–	8.98	10.83
($C_{31}H_{47}Cl_2NiN_3O_4$)	(56.81)	(7.23)	(6.41)	–	(8.96)	(10.82)
[Co(CQ)(Ibu)$(H_2O)_2$Cl]	56.79	7.25	6.44	–	8.94	10.85
($C_{31}H_{47}Cl_2CoN_3O_4$)	(56.75)	(7.23)	(6.41)	–	(8.99)	(10.82)
[Cu(CQ)(Ibu)$(H_2O)_2$Cl]	56.43	7.16	6.38	–	9.67	10.75
($C_{31}H_{47}Cl_2CuN_3O_4$)	(56.40)	(7.18)	(6.36)	–	(9.63)	(10.74)
[Zn(CQ)(Ibu)$(H_2O)_3$]	56.28	7.14	6.37	–	9.86	10.73
($C_{31}H_{47}Cl_2ZnN_3O4$)	(56.24)	(7.16)	(6.35)	–	(9.88)	(10.71)
[Ni(CQ)(SMX)$(H_2O)Cl_2$]	46.61	5.40	11.58	4.47	8.10	14.72
($C_{28}H_{37}Cl_3CuO_4N_6S$)	(46.66)	(5.45)	(11.66)	(4.45)	(8.14)	(14.76)
[Co(CQ)(SMX)$(H_2O)Cl_2$]	46.61	5.43	11.67	4.42	8.19	14.79
($C_{28}H_{39}Cl_3CoN_6SO_4$)	(46.64)	(5.45)	(11.66)	(4.45)	(8.17)	(14.75)
[Cu(CQ)(SMX)Cl_3]	45.31	5.09	11.27	4.30	8.60	19.01
($C_{28}H_{37}Cl_4CuO_3N_6S$)	(45.25)	(5.02)	(11.31)	(4.32)	(8.55)	(19.06)
[Zn(CQ)(SMX)Cl_3]	45.21	4.97	11.62	4.33	8.81	14.71
($C_{28}H_{37}Cl_4ZnN_6O_4S$)	(45.15)	(5.01)	(11.66)	(4.30)	(8.78)	(14.76)

3.1. The infrared spectra

The infrared spectrum of chloroquine was compared with that of the metal complex. It is reported (Otuokere *et al.*, 2019) that the vibration frequencies of NH and C=N of chloroquine occur at 3260 and 1580 cm^{-1}. Chloroquine in these complexes behaves as a neutral monodentate molecule, due to the nitrogen atom in the quinoline ring.

3.1.1. Infrared spectra of nickel (II), cobalt (II), copper (II) and zinc (II) complexes with chloroquine and ibuprofen

Ibuprofen was bidentate through the oxygen atoms in the carboxyl group. As a result, in these complexes (**Figs. S1–S4**), a metal ion is coordinated with each of the two ligands, ibuprofen and chloroquine (**Table S1**) summarizes the bonding site assignments, which are based on the following pieces of evidence. A wide band that was present in all complexes within the 3467–3195 cm^{-1} range has been assigned to ν(OH) and ν(NH), with ν(OH) appearing at 3388–3467 cm^{-1} and ν(NH) appearing at 3195–3220 cm^{-1} (Otuokere *et al.*, 2019). At 3451 cm^{-1}, ν(OH) in the ibuprofen–free ligand is visible. The coordination is confirmed by the absence of ν(OH) vibration (Abbas *et al.*, 2022). According to (Bamigboye *et al.*, 2020), coordinated water can be distinguished by the appearance of 880 and 522 cm^{-1}, respectively. The peak at 1709 cm^{-1}, previously ascribed to the free ibuprofen band of C=O stretching (Abbas *et al.*, 2022), has been shifted to 1722 cm^{-1}, indicating that coordination occurred at this position.

The stretch of C=N in free chloroquine is linked to the peak at 1580 cm^{-1} (Mohammad and Abdullah, *et al.*, 1984). This peak moved to 1458 cm^{-1}, indicating that the C=N functional group was involved in coordination. The C=N bond length grew because of the falling electron density, which in turn caused the vibration frequency to decrease. This change implies that the location of the quinoline ring in chloroquine caused coordination. For each of the M–O vibrations at 416–445 cm^{-1}, the Ni(II), Co(II), Cu(II), and Zn(II) complexes displayed a single weak band. The current evidence of υ(M–N) could not be brought into the IR data due to instrumental limitations in the 219–297 cm^{-1} region (Nakamoto, 1978).

3.1.2. Infrared spectra of nickel(II), cobalt(II), copper(II), and zinc(II) complexes with chloroquine and sulfamethoxazole

Using KBr discs to examine the infrared bands of free sulfamethoxazole, three distinct and strong bands were found at 3466, 3377, and 3298 cm^{-1}. These bands are the result of symmetric and asymmetric stretching vibrations of the aromatic amino group (NH_2) and sulfonamide (NH), respectively (Al–Noor *et al.*, 2014; Alosaimi, 2022; Chavda *et al.*, 2021). According to Torre *et al.* (2005) and Jamil *et al.* (2017), stretching vibrations of the S=O group were found at 1365 cm^{-1} and 1091 cm^{-1}, respectively. By stretching the phenyl ring (C=C) strong and sharp bands are generated at 1596 cm^{-1} and 1503 cm^{-1}. As shown in **Figs. S5 and S6**, the complexes have the same bands in the same location with the same wave number without shifting. However, the complex in **Fig. S7** shows only one band at 3443 cm^{-1}, with the other bands disappearing. Three bands overlap, resulting in the formation of a broadband and the elimination of the other bands.

The complex in **Fig. S8** contains a single broadband at 3453cm^{-1} for the same reason.

The S=O group stretching vibrations are asymmetric and symmetric at 1365 and 1091 cm^{-1}, respectively. Asymmetric and symmetric were found at 1383 cm^{-1} and 1076 cm^{-1}, respectively, for the molecule shown in **Fig. S5**. **Table S2** contains the remaining items. The M–O stretching vibrations in the 421–483 cm^{-1} region are responsible for the new bands in the complex spectra. Current evidence of υ(M–N) was not included in IR data due to an experimental limitation in the 219–297 cm^{-1} range (Nakamoto, 1978).

3.2. X–ray diffraction

3.2.1. X–ray diffraction of the chloroquine, ibuprofen ligands, and their complexes

Figure S9–S14 represent the XRD patterns for chloroquine, ibuprofen, and its complexes. From these figures, a notable shifting of the main peak toward higher diffraction angles (**Table S3**) is observed for the complexes, suggesting the reduction of the unit cell dimensions and consequently contracting the crystal lattice (Aroyo, 2016). In addition, significant changes in intensities of the main peaks of ligands and their complexes are observed in these figures, which are attributed to the reduction in crystallinity. The crystallinity calculations are based on the ratio of the principal peak area of the complex sample to that of the ligand sample, obtaining a relative crystallinity (Shah *et al.*, 2006). The results in **Table S3** show significant changes in crystallinity between chloroquine, ibuprofen, and its complexes that exhibit low relative crystallinity (3.201, 4.600, 23.017 and 24.366%). In the literature, the range between 1–100 nm is reported to be of nanoparticle size (Boverhof *et al.*, 2015). The particle size of the complexes obtained from XRD shows effects on their nanoparticle size (4.422, 2.99, 4.821 and 4.4054 nm).

3.2.2. X–ray diffraction of the chloroquine, sulphamethoxazol ligands, and their complexes

The XRD patterns for chloroquine, sulfamethoxazole, and their compounds are shown in **Fig. S15– S19**. According to these figures, a notable shift of the primary peak for the complexes towards higher diffraction angles (**Table S4**) suggests that the dimensions of the unit cells have decreased, which has caused the crystal lattice to constrict (Aroyo, 2016). Calculations of relative crystallinity are also based on the ratio of the primary peak area of the complex sample to that of the ligand sample (Shah *et al.*, 2006). The findings shown in **Table S4** demonstrate considerable variations in the relative crystallinity of chloroquine, sulfamethoxazole and their complexes (61.386, 23.513, 92.978 and 32.538%). The literature reports that the sizes of nanoparticles fall within the range of 1 to 100 nm (Boverhof *et al.*, 2015). The complexes discovered by XRD had nanoparticle–sized particles (5.058, 4.789, 3.5754 and 4.9042 nm). The proposed structure of the complexes in **Figs. 1** and **2**.

3.3 Biological effect of metal complexes against *Aedes aegypti* larvae

The larvicidal bioassay adhered to the established guidelines by the WHO (Abbott, 1925). Concentrations of 50, 100, 150, 300, 500, and 1000 ppm were prepared in 3% DMSO for each chemical. The late third or early fourth instar larvae were constantly exposed to different concentrations of chemicals for the duration of the treatments. Following these tests, the larvae were given their regular diet. The fatality percentage was reported after a 24–hour exposure period.

The compounds were carefully stored according to the recommended conditions by periodic measurements to assess their pH, solubility, and dissolution stability. DMSO solvent was employed to ensure the integrity of the compounds, avoiding any solvent that could potentially affect their properties. The compounds' physical appearance, including color and odor, were examined in addition to the physicochemical assessments. Comprehensive biological tests took place to evaluate their properties during the storage period. These experiments involved a wide range of concentrations at the beginning of the evaluation, and to determine the stability and shelf–life of these compounds high (1000 ppm) and low (50 ppm) concentrations were utilized. These concentrations were chosen after four months of storage, reflecting real–life conditions. By employing this approach, the compounds' long–term stability could be assessed and established their suitability for practical applications.

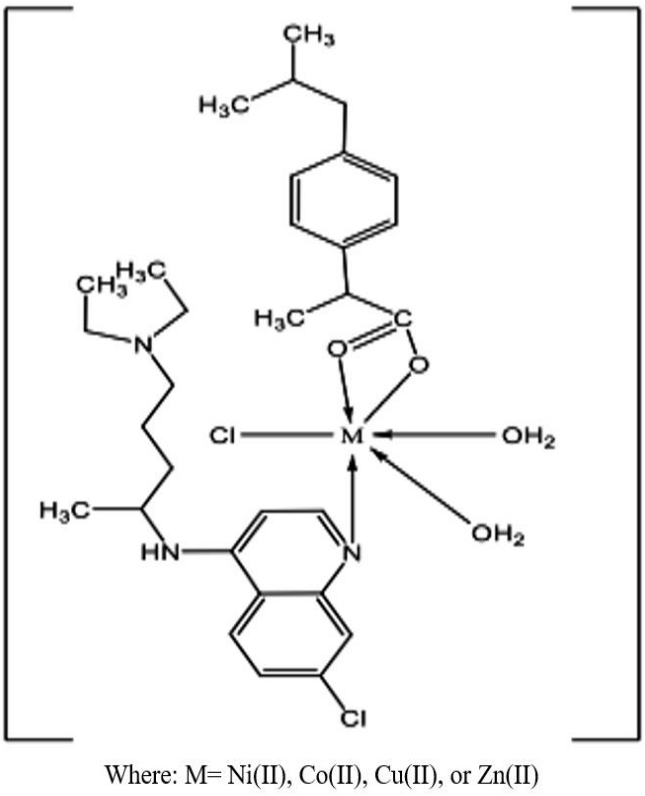

Figure 1. Proposed structure of (CQ)(Ibu) complexes.

https://doi.org/10.26850/1678-4618.eq.v49.2024.e1526

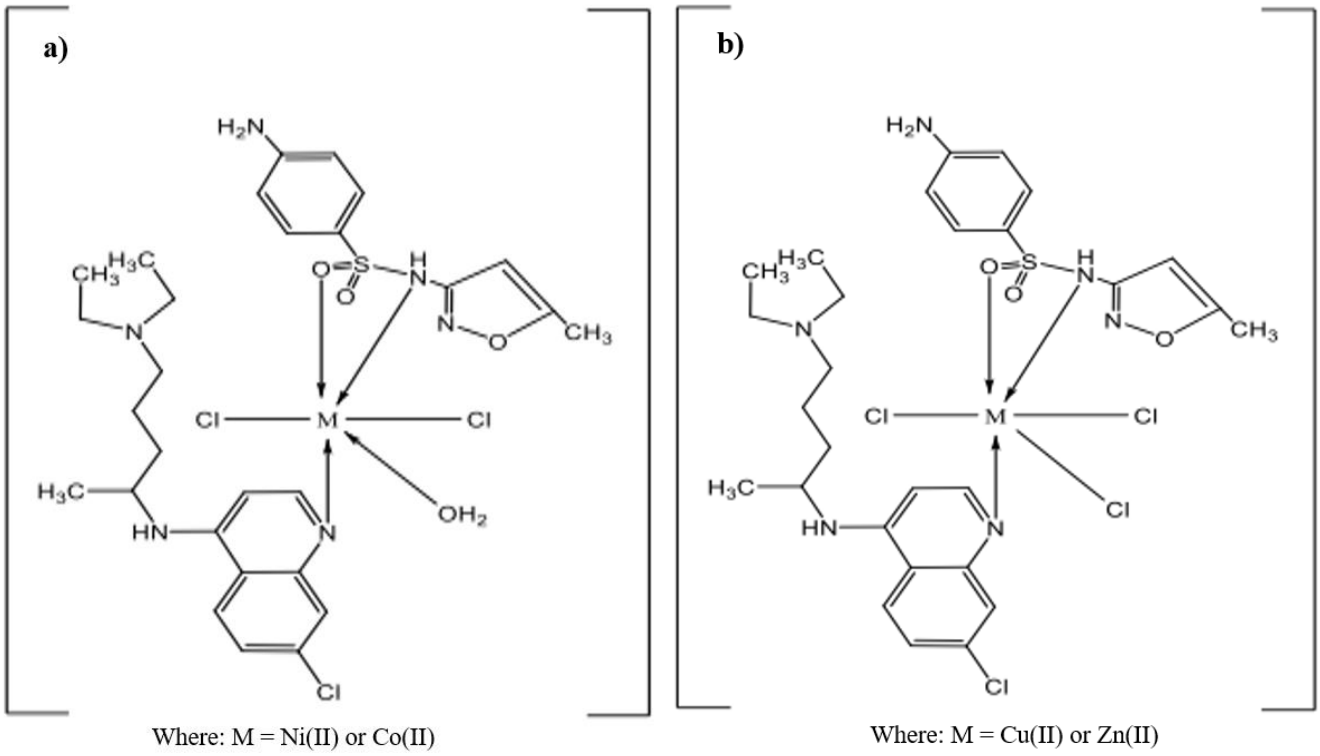

Figure 2. Proposed structure of (CQ)(SMX)complexes.

3.3.1 Statistical analysis

A complete randomized design (CRD) was used in a factorial experiment design. Using the Minitab application, the statistical analysis of the data was performed using analysis of variance (ANOVA) tools, and the averages were compared by Least Significance Difference LSD at $p \leq 0.05$. According to the Probit analysis program, LC_{50} (concentration that kills 50% of mosquito larvae) and LC_{95} (concentration that kills 95% of mosquito larvae) were determined (Abbott, 1925; Tisgratog *et al.*, 2016). According to an automated log–probit analysis, the 95% confidence interval.

3.3.2. Biological effect of the complexes nickel (II), cobalt (II), copper (II) and zinc (II) with chloroquine phosphate, and ibuprofen against larvae mosquito (*Aedes aegypti*)

As given in **Table S5** chloroquine, ibuprofen and their complexes with nickel (II), cobalt (II), copper (II) and zinc (II) were less effective in larvae mortality compared to the ibuprofen compound at concentrations of 1000 ppm and 300 ppm. For copper and zinc metal complexes, the percentage of mosquito larvae mortality was higher than that of the nickel (II) complex, and the cobalt (II) complex did not affect mosquito larvae. The acidic effect of the chloroquine diphosphate ligand resulting from the two phosphate groups is the main reason for the effectiveness, where the pH is (3.8 to 4.3). The effect of free Ibuprofen may be due to the carboxylic acid group of the acidic effect. It was also assumed that complexes with endogenous metals (Ni, Co, Cu, and Zn) could be less toxic than those with nonessential metals (WHO, 1999). Copper–containing coordination compounds were found to be promising therapeutic agents in a diverse range of diseases, including malaria, due to their ability to act by various mechanisms, such as inhibition of proteasome activity (WHO, 2003), telomerase activity (Meshnick and Dobson, 2001), and formation of reactive oxygen species (ROS) (Wells, 2011), DNA degradation (Stork *et al.*, 2001), and DNA intercalation (Wongsrichanalai *et al.*, 2002). All complexes are less acidic than their ligands due to chelation and changing of the –COOH group in ibuprofen into the –COO– group but, may have a high effect of some complexes against *Ae. aegypti.* depend on the toxicity of the metal (Rayms–Keller *et al.*, 1998).

The effectiveness of CQ,Ibu–Cu complexes increases with concentration (**Table 3**). The high effect of this complex against *Ae. aegypti* depends on the toxicity of the metal (Rayms–Keller *et al.*, 1998). Then, the toxicity line was drowned to calculate LC_{50} and LC_{95} (**Table 4** and **Fig. S20**).

Table 3. Toxicity effect of CQ,Ibu–Cu complex against *Ae. aegypti* larvae.

Compound	Conc. (ppm)	Larval Mortality (%)
CQ,Ibu–Cu complex	50	10
	100	17
	150	26
	300	70
	500	88
	1000	100
Control	3% DMSO	0

Table 4. Statistical parameters of CQ,Ibu –Cu complex.

Statistical parameters	CQ, Ibu–Cu complex
LC_{50} (ppm)	209.73
95% (*F. L)	198.48 – 221.09
LC_{95} (ppm)	609.12
95% (*F. L)	565.26 – 662.08
Slope	1.37
R^2	0.98

3.3.3. Biological effect of nickel (II), cobalt (II), copper (II) and zinc (II) complexes with chloroquine phosphate and sulfamethoxazole against larvae mosquito (*Aedes aegypti*)

Chloroquine, sulfamethoxazole and their complexes with nickel (II), cobalt (II), copper (II) and zinc (II) were less efficient in causing mortality in larvae than their complexes at concentrations of 1000 and 300 ppm, as shown in **Table S6**. Sulphamethoxazole ligand may have a basic effect in situations where it was not effective against larvae, and the effects of all subsequent ligands and complexes rely on acidity. The effectiveness of the CQ,SMX–Cu complex increased with concentration (**Table 5**). Depending on the metal's toxicity, this combination has a strong anti–*Aedes aegypti* action (Wongsrichanalai *et al.*, 2002). Then, the toxicity line was drowned to calculate LC_{50} and LC_{95} (Jamil *et al.*, 2023b) (**Table 6** and **Fig. S21**).

Table 5. Toxicity effect of CQ,SMX–Cu complex against *Ae. aegypti* larvae.

Compound	Concentration (ppm)	Larval Mortality (%)
CQ SMX–Cu Complex	50	30
	100	50
	150	68
	300	80
	500	85
	1000	100
Control	3% DMSO	0

Table 6. Statistical parameters of CQ,SMX–Cu complex.

Statistical parameters	CQ,SMX–Cu complex
LC_{50} (ppm)	103.12
95% (*F. L)	92.56 – 113.51
LC_{95} (ppm)	699.39
95% (*F. L)	622.64 – 799.36
Slope	0.76
R^2	0.94

4. Conclusions

The novel compounds have been produced by mixing chloroquine phosphate with ibuprofen and sulfamethoxazole, individually with the metals Ni(II), Co(II), Cu(II) and Zn(II). This research has looked at how the ligands and their complexes affect *Ae. aegypti* mosquito larvae biologically. Based on these findings, it was determined that the mixed ligand complexes have beneficial effects against the larval stage of *Ae. aegypti*. The most effective compounds were Cu(II) complexes, followed by Ni(II), Co(II), and Zn(II) complexes. The Cu(II) complexes may offer other strategies for limiting the *Ae. aegypti* mosquito, the dengue vector, according to this study's findings. These findings could motivate researchers to look for new active substances that could be effective substitutes for the present pesticides.

Authors' contributions

Conceptualization: Jamil, Y. M.; Al–Azab, F. M.; Al–Ryami, A. M.; **Data curation:** Al–Ryami, A. M.; **Formal Analysis:** Jamil, Y. M.; Al–Ryami, A. M.; Al–Selwi, N. A.; **Funding acquisition:** Not applicable; **Investigation:** Jamil, Y. M.; Al–Azab, A. M.; Al–Ryami, A. M.; **Methodology:** Jamil, Y. M.; Al–Azab, A. M.; Al–Ryami, A. M.; **Project administration:** Jamil, Y. M.; **Resources:** Jamil, Y. M.; Al–Azab, F. M.; Al–Azab, A. M.; **Software:** Jamil, Y. M.; Al–Azab, A. M.; Al–Ryami, A. M.; **Supervision:** Jamil, Y. M.; Al–Azab, F. M.; **Validation:** Jamil, Y. M.; Al–Azab, F. M.; **Visualization:** Jamil, Y. M.; Al–Azab, F. M.; Al–Selwi, N. A.; **Writing – original draft:** Al–Ryami, A. M.; Al–Selwi, N. A.; **Writing – review & editing:** Jamil, Y. M.

Data availability statement

The data will be available upon request.

Funding

Not applicable.

Acknowledgments

Not applicable.

References

Abbas, A. M.; Aboelmagd, A.; Kishk, S. M.; Nasrallah, H. H.; Boyd, W. C.; Kalil, H. and Orabi, A.S. A Novel Ibuprofen Derivative and Its Complexes Physicochemical Characterization, DFT Modeling, Docking, In Vitro Anti–Inflammatory Studies, and DNA Interaction. *Molecules*. **2022**, *27* (21), 7540. https://doi.org/10.3390/molecules27217540

Abbott, W. S. A Method of Computing the Effectiveness of an Insecticide. *Journal of Economic Entomology*. **1925**, *18* (2), 265–267. https://doi.org/10.1093/jee/18.2.265a

Adediji, J. F.; Olayinka, E. T.; Adebayo, M. A.; Babatunde, O. A study of the mode of coordination of mixed antimalarial metal complexes. *African Journal of Malaria and Tropical Diseases*. **2018**, *6* (10), 444–449.

Al–Azab, A. M.; Zaituon, A. A.; Al–Ghamdi, K. M.; Abd Al–Galil, F. M. Effect of Four Indigenous Medicinal Plants on Dengue Fever, Vector *Aedes aegypti* from Jeddah, Saudi Arabia. *Biosc. Biotech. Res. Comm*. **2020,** *13* (1), 212–218. https://doi.org/10.21786/bbrc/13.1/37

Al–Noor, T. H.; Mahdi, R. T.; Ismael, A. H. Preparation, characterization, and antibacterial properties of mixed ligand complexes of L–aspargine and sulfamethoxazole(antibiotic) with Mn(II), Co(II), Ni(II), Cu(II), Zn(II), Cd(II) and Hg(II) ions. *Journal of Chemical and Pharmaceutical Research*. **2014**, *6* (5), 1286–1294. https://doi.org/10.18488/journal.65/2014.1.6/65.6.109.120

Alosaimi, E. H. Spectroscopic Characterization, Thermogravimetry and Biological Studies of Ru(III), Pt(IV), Au(III) Complexes with Sulfamethoxazole Drug Ligand. *Crystals*. **2022**, *12* (3), 340. https://doi.org/10.3390/cryst12030340

Alyousefi, T. A. A.; Abdul–Ghani, R.; Mahdy, M. A. K.; Al–Eryani, S. M. A.; Al–Mekhlafi, A. M.; Raja Y. A.; Shah, S. A.; Beier, J. C. A household–based survey of knowledge, attitudes and practices towards dengue fever among local urban communities in Taiz Governorate, *Yemen. BMC Infect Dis*. **2016**, *16* (1), 543. https://doi.org/10.1186/s12879–016–1895–2

Aroyo, M. I. *International Tables for Crystallography Volume A*: Space–Group Symmetry. John Wiley and Sons, 2016. https://doi.org/10.1107/97809553602060000114

Bader, N. R. Sample preparation for flame atomic absorption spectroscopy: an overview. RJC. **2011**, *4* (1), 49–55.

Bamigboye, O. M.; Ejidike, I. P.; Ahmed, R. N.; Lawal, M.; Nnabuike, G. G. Medubi, K. Chelation, characterization, and antibacterial activities of some mixed isonicotinic acid hydrazide–Paracetamol metal drug complexes. *Suranaree J. Sci. Technol.* **2020,** *27* (3), 030026.

Bar, A.; Andrew, J. Morphology and Morphometry of *Aedes aegypti* Larvae. *Annual Review & Research in Biology*. **2013**, *3* (1), 1–21.

Bhatt, S.; Gething, P. W.; Brady, O. J.; Messina, J. P.; Farlow, A. W.; Moyes, C. L.; Drake, J. M.; Brownstein, J. S.; Hoen, A. G.; Sankoh, O.; Myers, M. F.; George, D. B.; Jaenisch, T.; Wint, G. R. W.; Simmons, C. P.; Scott, T. W.; Farrar, J. J.; Simon I. Hay, S. I. The global distribution and burden of dengue. *Nature*. **2013**, *496*, 504–507. https://doi.org/10.1038/nature12060

Bin Ghouth A. S. B.; Amarasinghe, A.; Letson, G. W. Dengue outbreak in Hadramout, Yemen, 2010: an epidemiological perspective. *Am J Trop Med Hyg*. **2012**, *86* (6),1072. https://doi.org/10.4269/ajtmh.2012.11–0723

Biot, C.; Nosten, F.; Fraisse, L.; Ter–Minassian, D.; Khalife, J.; Dive, D. The antimalarial ferroquine: From bench to clinic. *Parasite*, **2011**, *18*, 207–214. https://doi.org/10.1051/parasite/2011183207

Boverhof, D. R.; Bramante, C. M.; Butala, J. H.; Clancy, S. F.; Lafranconi, M.; West, J.; Gordon, S. C. Comparative assessment of nanomaterial definitions and safety evaluation considerations. *Regulatory Toxicology and Pharmacology*. **2015**, *73* (1), 137–150. https://doi.org/10.1016/j.yrtph.2015.06.001

Charrel, R. N.; Leparc–Gofart, I.; Gallian, P.; Lamballerie, X. Globalization of chikungunya: 10 years to invade the world. *Clin Microbiol Infect*. **2014**, *20* (7), 662–663. https://doi.org/10.1111/1469-0691.12694

Chavda, B. R.; Socha, B. N.; Pandya, S. B.; Chaudhary, K. P.; Padariya, T. J.; Alalawy, M. D.; Patel, M. K.; Dubey, R. P.; Patel, U. H. Coordination behavior of dinuclear silver complex of sulfamethoxazole with solvent molecule having static rotational d isorder: Spectroscopic characterization, crystal structure, Hirshfeld surface and antimicrobial activity. *J. Mol. Struct*. **2021**, *1228*, 129777. https://doi.org/10.1016/j.molstruc.2020.129777

Chew, T.; Pakasi, T.; Taylor–Robinson, A**.** Dengue Infection in Indonesia: Improved Clinical Profiling is Needed to Better Inform Patient Management and Disease Outbreak Control. *Journal of Tropical Medicine and Health*. **2019,** *3*, 142. https://doi.org/10.29011/2688-6383.000042

David, M. R.; Dantas, E. S.; Maciel–de–Freitas, R.; Codeço, C. T.; Prast, A. E.; Lourenço–de–Oliveira, R. Influence of Larval Habitat Environmental Characteristics on Culicidae Immature Abundance and Body Size of Adult Aedes Aegypti. *Front. Ecol. Evol*. **2021**, *9*, 626757. https://doi.org/10.3389/fevo.2021.626757

Fauci, A. S.; Morens, D. M. Zika virus in the Americas—yet another arbovirus threat. *New Eng Jour Med.* **2016**, *374* (7), 601–604. https://doi.org/10.1056/nejmp1600297

Gutu, M. A.; Bekele, A.; Seid, Y.; Mohammed, Y.; Gemechu, F.; Woyessa, A. B.; Tayachew, A.; Dugasa, Y.; Gizachew, L.; Idosa, M.; Tokarz, R. E.; Sugerman, D. Another dengue fever outbreak in eastern Ethiopia—an emerging public health threat. *PLOS Negl Trop Dis*. **2021**, *15* (1), e0008992. https://doi.org/10.1371/journal.pntd.0008992

Jamil, Y. M. S.; Al–Maqtari, M. A.; Al–Qadasi, M. K. Ligational and Spectroscopic On Some Sulfamethoxazole Metal Complexes As Antimicrobial Agents, *European Journal Of Pharmaceutical And Medical Research*. Ejpmr. **2017**, *4* (7), 95–105.

Jamil, Y. M. S.; Al–Azab, F. M.; Al–Selwi, N. A.; Alorini, Th. and Al–Hakimi, A. N. P. Preparation, physicochemical characterization, molecular docking and biological activity of a novel schiff–base and organophosphorus schiff base with some transition metal(II) ions. *Main Group Chemistry*. **2022a**, 1–26. https://doi.org/10.3233/MGC-220101

Jamil, Y. M. S.; Al–Azab, F.; Al–Selwi, N.; Al–duais, F.; Al–Hakimi, A.; Alhagri, I.; El–Sayed, S. Synthesis, Spectroscopic and Antibacterial Studies of New Schiff–base and Organophosphorus Schiff–base with Some Transition Metal (II) Ions. *Journal of Qassim University for Science*. **2022b**, *1* (1), 129–153.

Jamil, Y. M. S.; Al–Azab, F. M.; Al–Selwi, N. A. Novel organophosphorus schiff base ligands: synthesis characterization, ligational aspcts, XRD and biological activity studies. *Eclét. Quím*. **2023a**, *48* (3), 36–53. https://doi.org/10.26850/1678-4618eqj.v48.3.2023.p36-53

Jamil, Y. M. S.; Al–Azab, A.; Al–Azab, F.; Al–Selwi, N. A. Larvicidal Effects of New Organophosphorus Schiff base compounds against Dengue Fever Vector Aedes aegypti (Diptera; Culicidae). *Sana'a University Journal of Applied Sciences and Technology* **2023b**, 1(1) 78 – 87. https://doi.org/10.59628/jast.v1i1.156

Jasim, D. J.; Abbas, A. K. Synthesis, identification, antibacterial, medical and dying performance studies for azosulfamethoxazole metal complexes. *Eurasian Chem. Commun*. **2022**, *4*, 16–40. https://doi.org/10.22034/ecc.2022.310593.1251

Kucharski, D. J.; Jaszczak, M. K.; Przemysław Boraty´nski, J. A. Review of Modifications of Quinoline Antimalarials Mefloquine and (hydroxy)Chloroquine. *Molecules*. **2022**, *27* (3), 1003. https://doi.org/10.3390/molecules27031003

Kumar, K. S.; Reena, V. N.; Aravindakshan, K. K. Synthesis, anticancer and larvicidal activities of a novel Schiff base ligand, 3–((2–((1–(4–hydroxyphenyl)ethylidene)amino)ethyl)imino)–N–(p–tolyl) butanamide and its Mn(II), Fe(III), Co(II), Ni(II) and Zn(II) complexes. *Results in Chemistry*, **2021**, *3*, 100166. https://doi.org/10.1016/j.rechem.2021.100166

Leandro, A. D. S.; Ayala, M. J. C.; Lopes, R. D.; Martins, C. A.; Maciel–de–Freitas R.; Villela, D. A. M. Entomo–Virological *Aedes aegypti* Surveillance Applied for Prediction of Dengue Transmission: A SpatioTemporal Modeling Study. *Pathogens*. **2023**, *12* (1), 4. https://doi.org/10.3390/pathogens12010004

Maciel-de-Freitas, R.; Marques, W. A.; Peres, R. C.; Cunha, S. P.; Lourenço-de-Oliveira, R. Variation in *Aedes aegypti* (Diptera: Culicidae) Container Productivity in a Slum and a Suburban District of Rio de Janeiro during Dry and Wet Seasons. *Mem. Inst. Oswaldo Cruz*. **2007**, *102*, 489–496. https://doi.org/10.1590/s0074–02762007005000056

Marcondes, C. B.; Ximenes, F. F. M. Zika virus in Brazil and the danger of infestation by *Aedes (Stegomyia)* mosquitoes. *Rev. Soc. Bras. Med. Trop*. **2015**, *49* (1), 4–10. https://doi.org/10.1590/0037-8682-0220-2015

Meshnick, S. R.; Dobson, M. J. The history of antimalarial drugs. Antimalarial chemotherapy. *P. J. Rosenthal (ed.)*. **2001**, 15–26. https://doi.org/10.1385/1-59259-111-6:15

Mohammad, T.; Abdullah, A. *Analytical profiles of drug substances*. King Saud University, 1984.

Muthuppalani, M.; Al Otaibi, A.; Balasubramaniyan, S.; Manikandan, S.; Manimaran, P.; Mathubala, G.; Manikandan, A.; Arshad, M. N.; Puttegowda, M.; Alorfi, H. S.; Khan, A.; Asiri, A. M.; Rahman, M. M. Synthesis, Characterization and Bio–Potential Activities of Co(II) and Ni(II) Complexes with O and N Donor Mixed Ligands. *Crystals*, **2022**, *12* (3), 326. https://doi.org/10.3390/cryst12030326

Nakamoto, K. *Infrared and Raman Spectra of Inorganic and Coordination Compounds*. John Wiley and Sons, 1978.

Netoi, A.; Junior, P.; Silva, M.; Lima, S.; Yara, R.; Guimavaes, E.; Santana, E.; Selva, L.; Delira, E.; Vieir, J. Evaluation of Embryotoxic and Embryostatic Effects of the Aqueous Extract of Rhizophora mangle and Tannic Acid on Eggs and Larvae of *Aedes aegypti*. *Anais da Academia Brasileira de Ciencias*. **2018**, *2* (1), 2141–2148. https://doi.org/10.1590/0001–3765201720170297

Otuokere, I. E.; Okpara, L. O.; Amadi, K. C.; Alisa,C. O.; Okoyeag, A.; Nwadire, F. C. Synthesis, Characterization and Complexation Behaviour of Chloroquine towards Ti (II) Ion. *Journal of Pharmaceutical Research International*. **2019**, *27* (3), 1–6. https://doi.org/10.9734/jpri/2019/v27i330168

Patterson, A. The Scherrer formula for X–ray particle size determination. *Phys. Rev*. **1939**, *56*, 978. https://doi.org/10.1103/PhysRev.56.978

Rajaganesh, R.; Murugan, K.; Panneerselvam, C.; Jayashanthini, S.; Roni, M.; Suresh, U.; Trivedi, S.; Rehman, H.; Higuchi, A.; Nicoletti, M.; Benelli, G. Fern–synthesized silver nanocrystals: Towards a new class of mosquito oviposition deterrents. *Res. Vet. Sci*. **2016**, *109*, 40–51. https://doi.org/10.1016/j.rvsc.2016.09.012

Rauseo, J.; Barra Caracciolo, A.; Ademollo, N.; Cardoni, M.; Di Lenola, M.; Gaze, W.; Stanton, I.; Grenni, P.; Pescatore, T.; Spataro, F.; Patrolecco, L. Dissipation of the antibiotic sulfamethoxazole in a soil amended with anaerobically digested cattle manure. *Mater*. **2019**, *378*, 120769. https://doi.org/10.1016/j.jhazmat.2019.120769

Rayms–Keller, A.; Olson, K. E.; McGaw, M.; Oray, C.; Carlson, J. O.; Beaty, B. J. Effect of Heavy Metals on Aedes aegypti (Diptera: Culicidae) Larva. *Ecotoxicology and environmental safety*. **1998,** *39* (1), 41–47. https://doi.org/10.1006/eesa.1997.1605

Refat, M. S.; Al-Azab F. M.; Al-Maydama H. M.; Amin R. R.; Jamil, Y.M.S. Synthesis and in vitro microbial evaluation of La(III), Ce(III), Sm(III) and Y(III) metal complexes of vitamin B6 drug. *Spectrochim. Acta - A: Mol. Biomol. Spectrosc.* **2014** *127* (2014) 196–215. https://doi.org/10.1016/j.saa.2014.02.043

Saeed, M.; Alenad, A. A.; Malik, M. A. Synthesis of mackinawite FeS thin films from acidic chemical baths. *Materials Science in Semiconductor Processing*. **2015**, *32*, 1–5. https://doi.org/10.1016/j.mssp.2014.12.073

Schrauf, S.; Tschismarov, R.; Tauber, E.; Ramsauer, K. Current eforts in the development of vaccines for the prevention of Zika and chikungunya virus Infections. *Front Immunol*. **2020**, *11*, 592. https://doi.org/10.3389/fimmu.2020.00592

Scott, T. W.; Chow, E.; Strickman, D.; Kittayapong, P.; Wirtz, R. A.; Lorenz, L. H.; Edman, J. D. Blood–Feeding Patterns of *Aedes aegypti* (Diptera: Culicidae) Collected in a Rural Thai Village. *J. Med. Entomol*. **1993**, *30*, 922–927. https://doi.org/10.1093/jmedent/30.5.922

Shah, B.; Kakumanu, V. K.; Bansal, A. K. Analytical techniques for quantification of amorphous/crystalline phases in pharmaceutical solids. *J. Pharm Sci*. **2006**, *95* (8), 1641–1665. https://doi.org/10.1002/jps.20644

Simmons, C.; Farrar, J. Changing Patterns of Dengue Epidemiology and Implications for Clinical Management and Vaccines. *PLoS Med*. **2009**, *6* (9), e1000129. https://doi.org/10.1371/journal.pmed.1000129

Singh, V. Metal complexes as antimalarial potential: A review. *The Pharma Innovation Journal.* **2019**, *8* (5), 403–406.

Singh, A.; Sharma, J.; Paichha, M.; Chakrabarti, R. *Achyranthes aspera* (prickly chaff flower) leaves- and seeds-supplemented diets regulate growth, innate immunity, and oxidative stress in *Aeromonas hydrophila*-challenged *Labeo rohita*. *J. Appl. Aquacult*. **2020**, 32 (3), 250-267. https://doi.org/10.1080/10454438.2019.1615594

Stork, G.; Niu, D.; Fujimoto, A.; Koft, E. R.; Balkovec, J. M.; Tata, J. R.; Dake, G. R. The first stereoselective total synthesis of quinine. *Journal of the American Chemical Society.* **2001**, *123* (14), 3239–3242. https://doi.org/10.1021/ja004325r

Suresh, U.; Murugan, K.; Benelli, G.; Nicoletti, M.; Barnard, D. R.; Panneerselvam, C.; Kumar, P. M.; Subramaniam, J.; Dinesh, D.; Chandramohan, B. Tackling the growing threat of dengue: Phyllanthus nirurimediated synthesis of silver nanoparticles and their mosquitocidal properties against the dengue vector *Aedes aegypti* (Diptera: Culicidae). *Parasitol Res.* **2015**, *114* (4), 1551–1562. https://doi.org/10.1007/s00436–015–4339–9

Szafran, Z.; Pike, R. M.; Singh, M. M. *Microscale inorganic chemistry*. John Wiley & Sons, 1991.

Tisgratog, R.; Sanguanpong, U, Grieco, J. P.; Ngoen–Kluan, R.; Chareonviriyaphap, T. Plants traditionally used as mosquito repellents and the implication for their use in vector control. *Acta Tropica.* **2016**, *157*, 136–144. https://doi.org/10.1016/j.actatropica.2016.01.024

Torre, M.; Calvo, S.; Pardo, H.; Mombru, A. W. Synthesis, spectroscopic characterization and crystal structure of disulfamethoxazole diaquo Ni(II) monohydrate. *J. Coord. Chem*. **2005**, *58* (6), 513–520. https://doi.org/10.1080/00958970500037516

Wells, T. N. C. Natural products as starting points for future anti–malarial therapies: going back to our roots. *Malaria Journal*. **2011**, *10* (1), 1–12. https://doi.org/10.1186/1475–2875–10–S1–S3

Wongsrichanalai, C.; Pickard, A. L.; Wernsdorfer, W. H.; Meshnick, S. R. Epidemiology of drug–resistant malaria. *The Lancet Infectious Diseases*. **2002**, *2* (4), 209–218. https://doi.org/10.1016/s1473–3099(02)00239–6

World Health Organization [WHO]. Weekly Epidemiological Record – Malaria, (1982–1997); Technical Report Number 32. Geneva: WHO, 1999. http://www.who.int/wer. Accessed 9 Sept. 2021

World Health Organization [WHO]. UNICEF. The Africa Malaria Report. Geneva: WHO, 2003. https://iris.who.int/handle/10665/67869. Accessed 9 Sept. 2021

World Health Organization [WHO]. Dengue and dengue haemorrhagic fever. Factsheet N°117. Geneva: WHO, 2008.

World Health Organization [WHO]. Dengue Guidelines for diagnosis, treatment, prevention and control 2009. Geneva: WHO, 2009. https://iris.who.int/handle/10665/44188. Accessed 9 Sept. 2021

https://doi.org/10.26850/1678-4618.eq.v49.2024.e1526

Supplementary Material

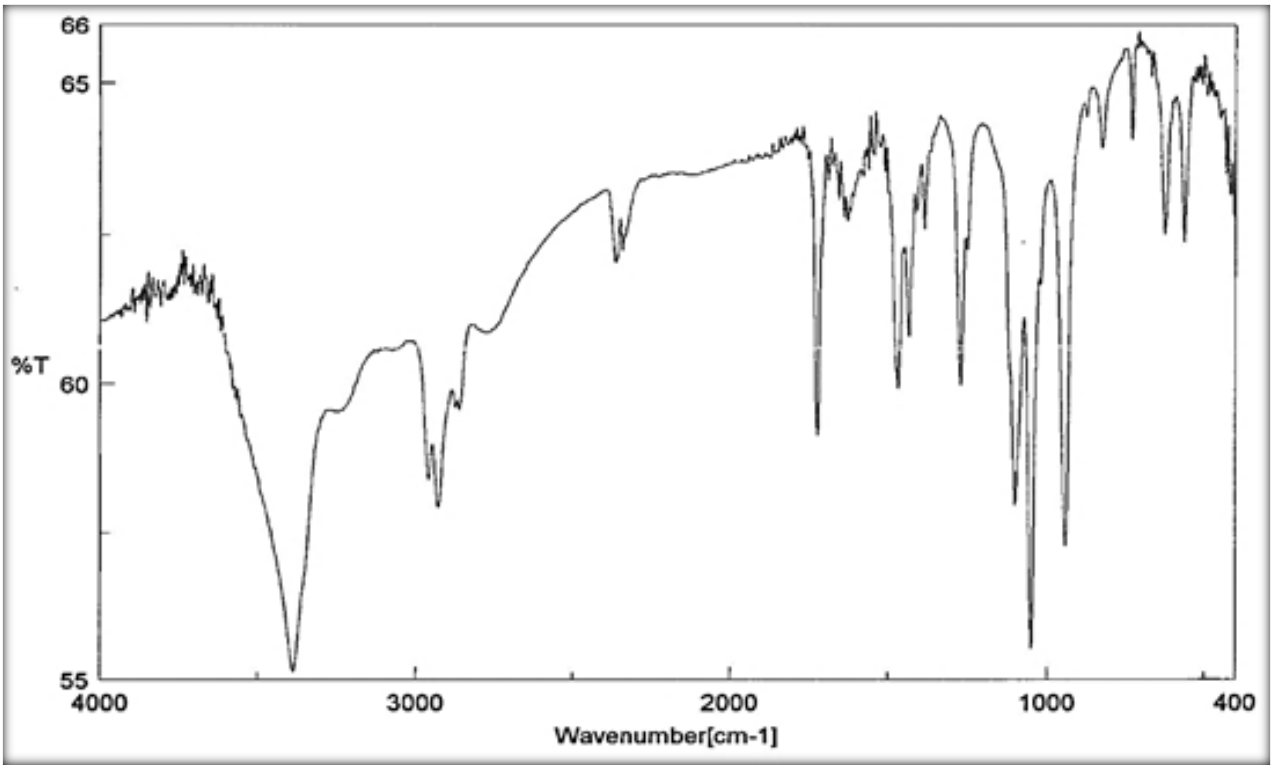

Figure S1. Infrared Spectrum of [Ni(CQ)(Ibu)$(H_2O)_2$Cl]complex.

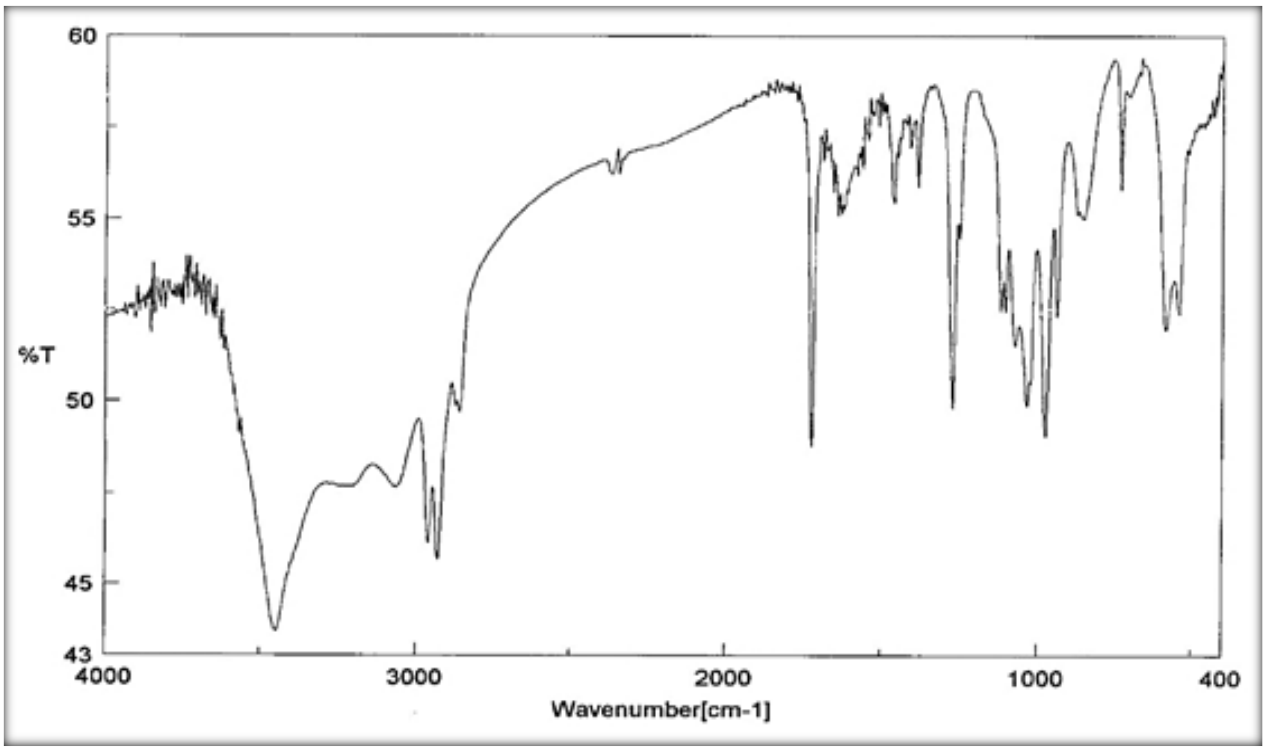

Figure S2. Infrared Spectrum of [Co(CQ)(Ibu)$(H_2O)_2$Cl]complex.

https://doi.org/10.26850/1678-4618.eq.v49.2024.e1526

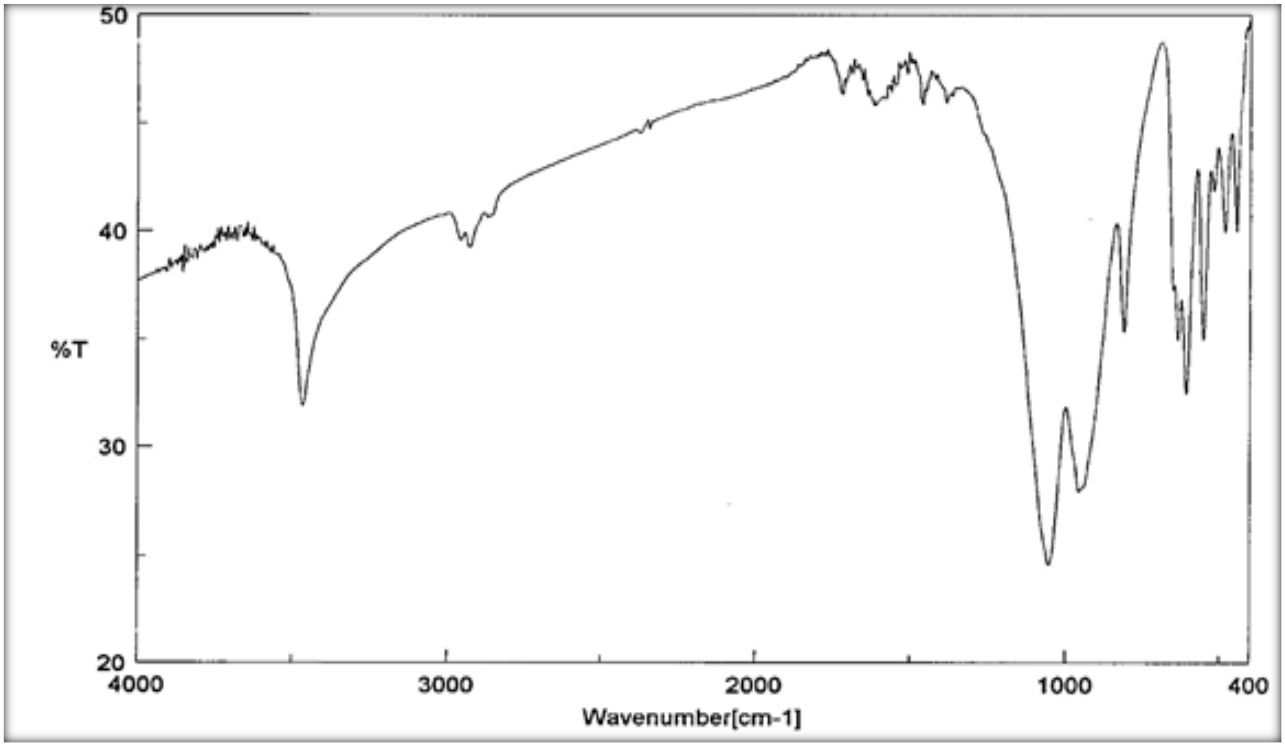

Figure S3. Infrared Spectrum of [Cu(CQ)(Ibu)$(H_2O)_2$Cl]complex.

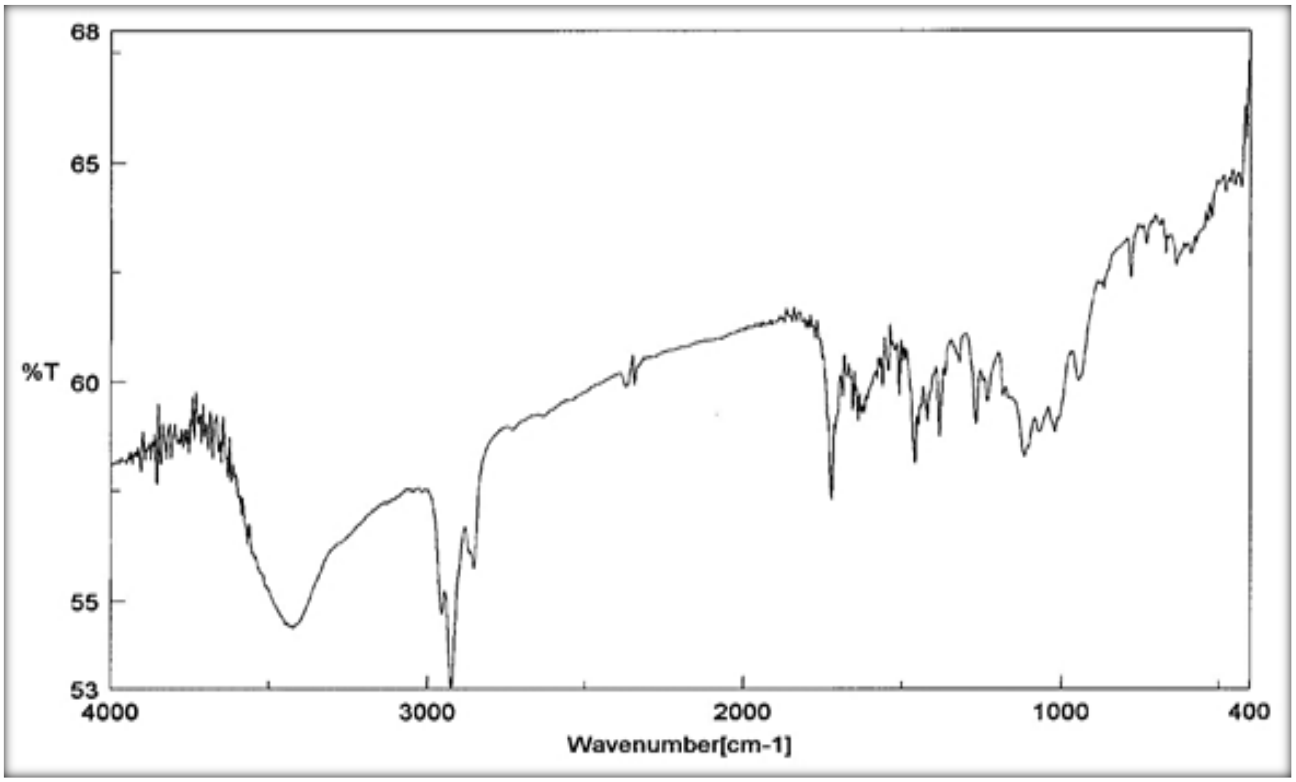

Figure S4. Infrared Spectrum of [Zn(CQ)(Ibu)$(H_2O)_2$Cl]complex.

https://doi.org/10.26850/1678-4618.eq.v49.2024.e1526

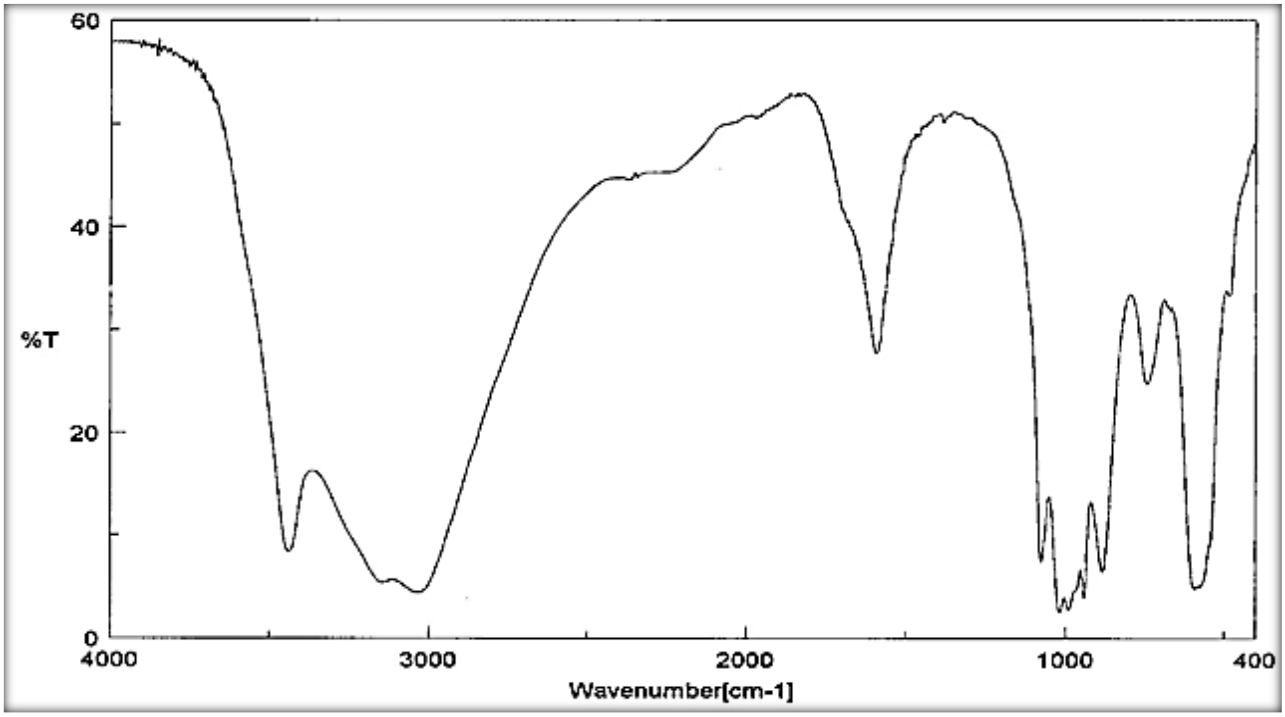

Figure S5. Infrared Spectrum of [Ni(CQ)(SMX)(H_2O)Cl_2] complex.

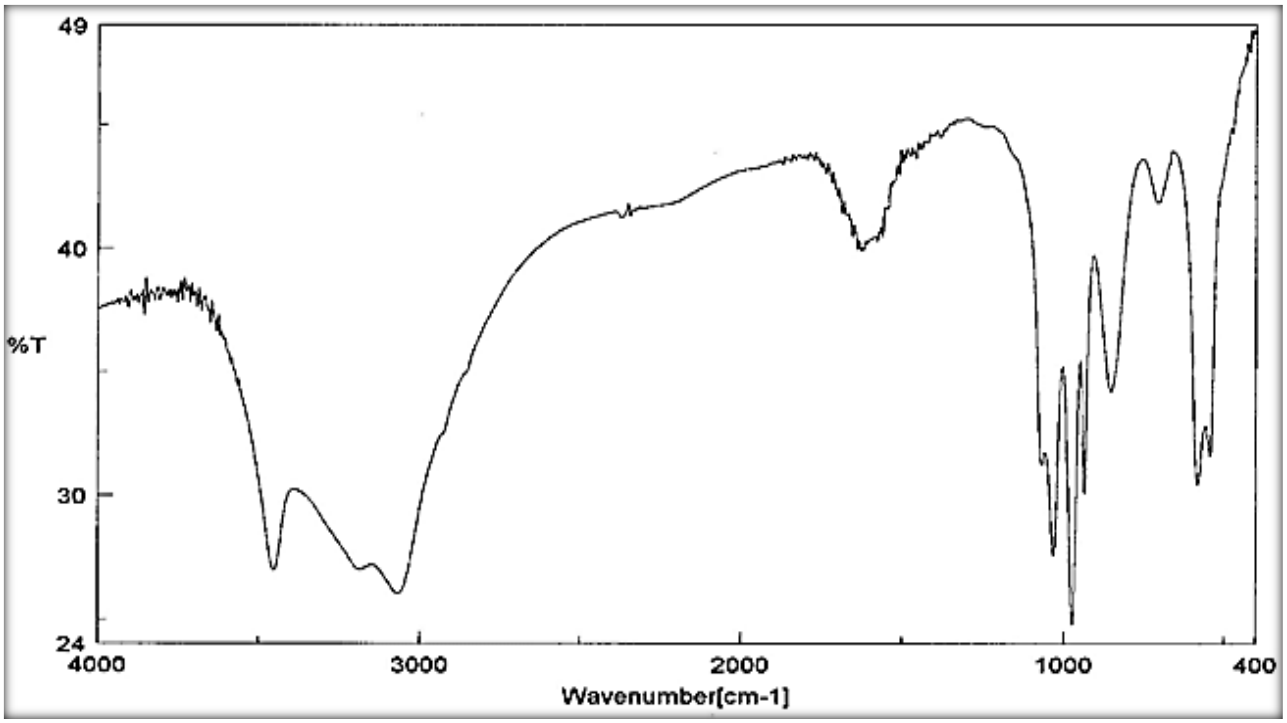

Figure S6. Infrared Spectrum of [Co(CQ)(SMX)(H_2O)Cl_2] complex.

https://doi.org/10.26850/1678-4618.eq.v49.2024.e1526

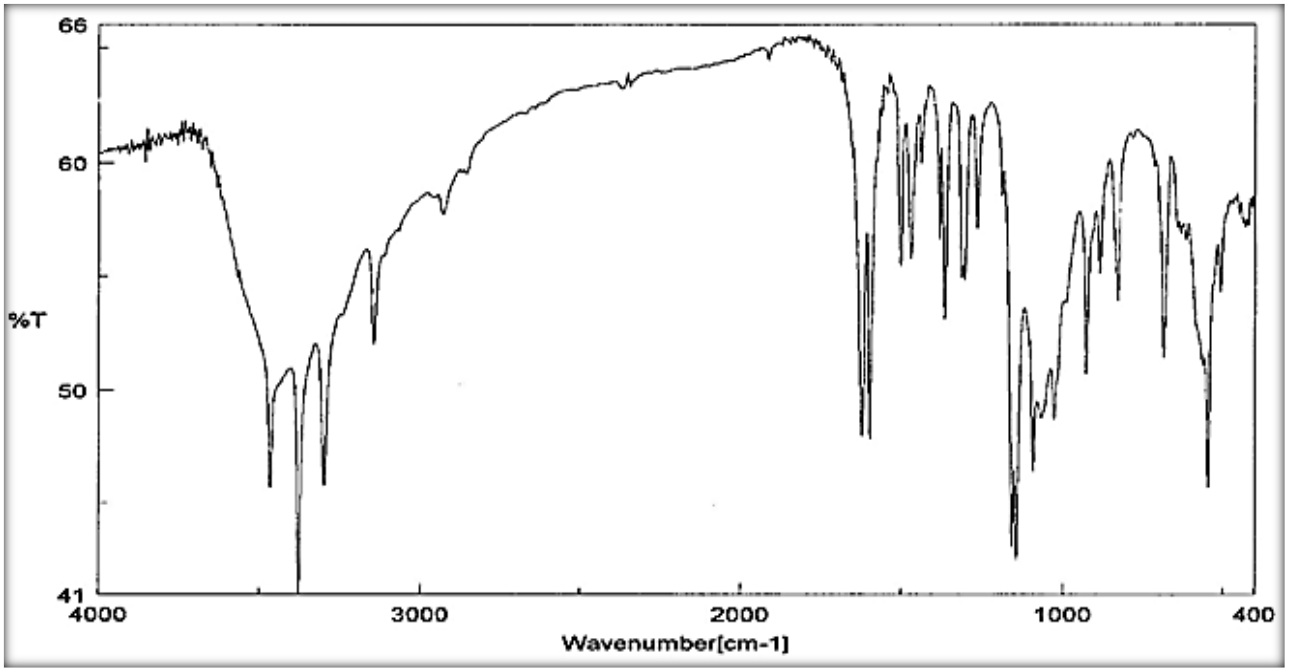

Figure S7. Infrared Spectrum of [Cu(CQ)(SMX)Cl_3] complex.

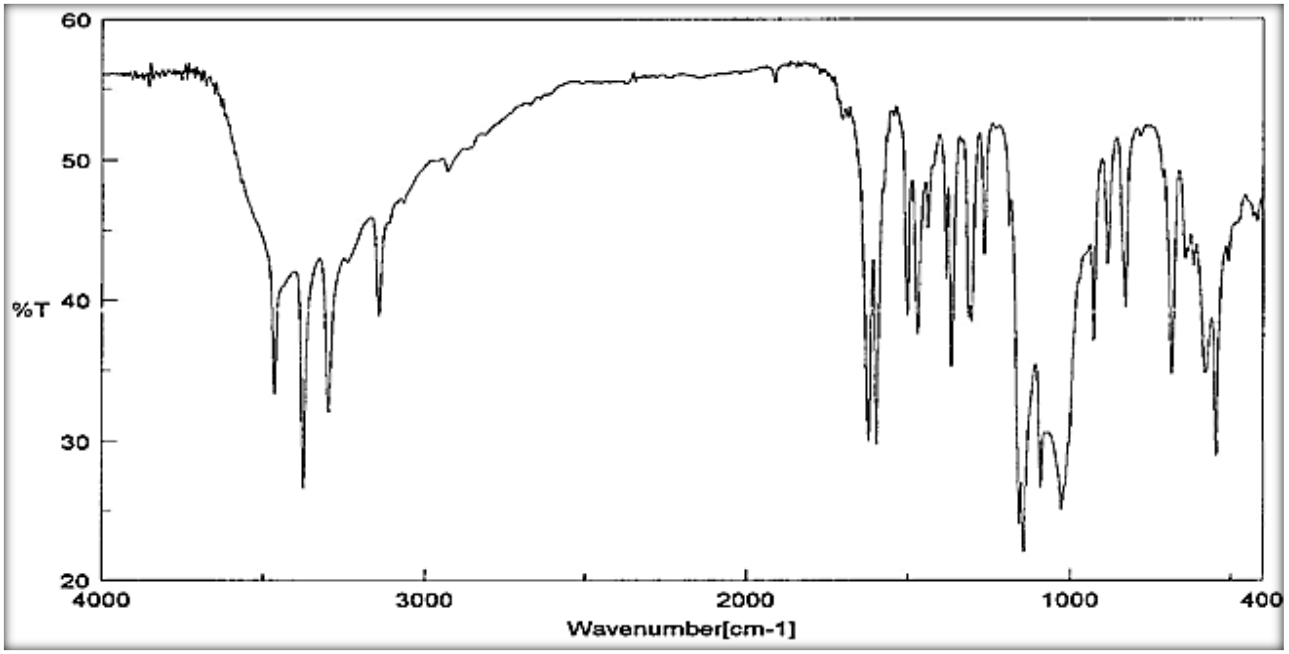

Figure S8. Infrared Spectrum of [Zn(CQ)(SMX)Cl_3] complex.

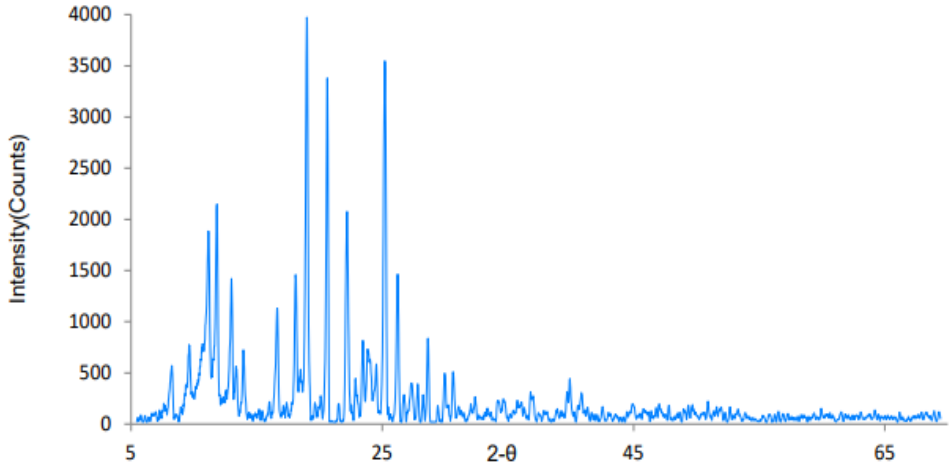

Figure S9. XRD pattern for chloroquine phosphate.

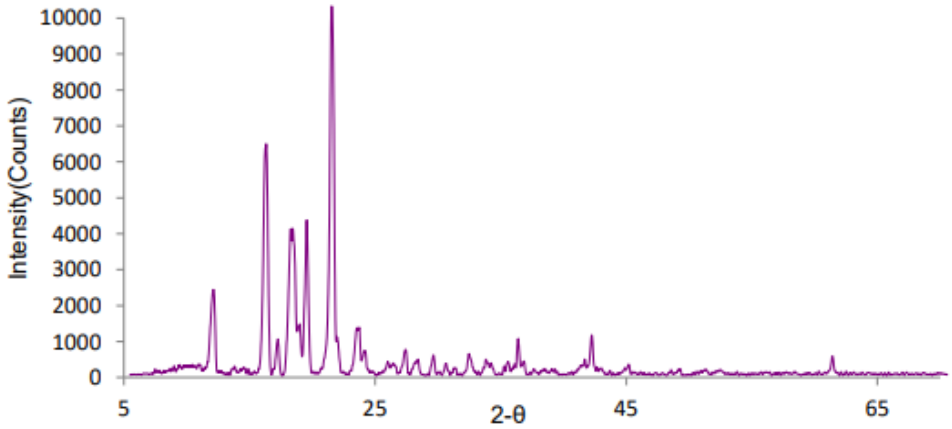

Figure S10. XRD pattern for ibuprofen.

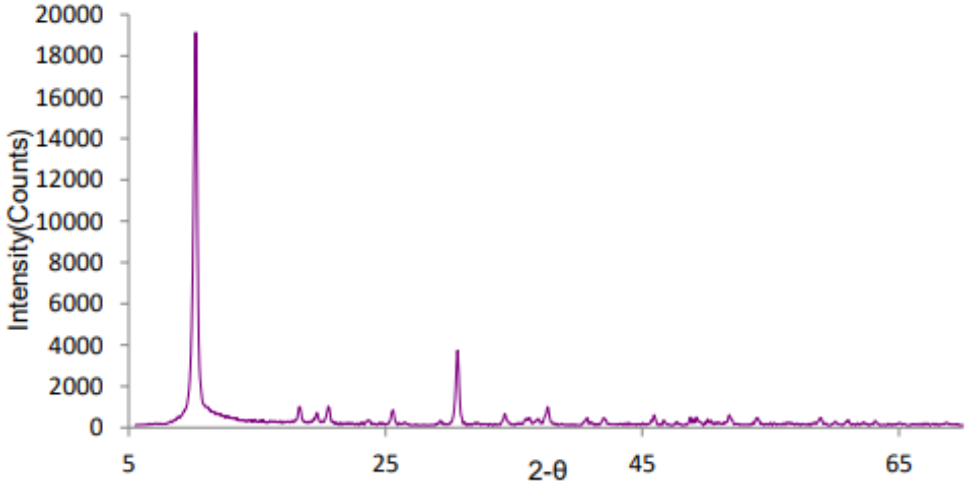

Figure S11. XRD pattern for CQ,Ibu-Ni complex.

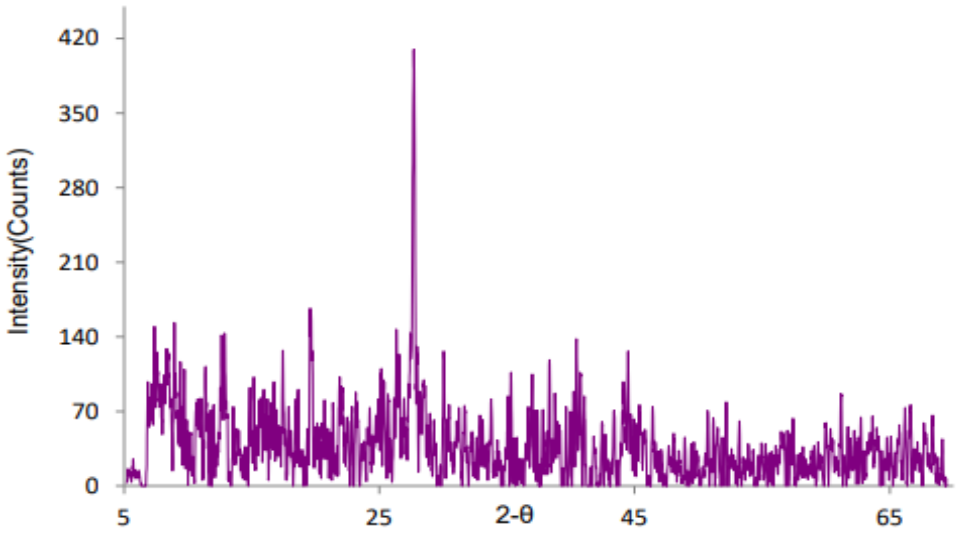

Figure S12. XRD pattern for CQ,Ibu-Co.complex.

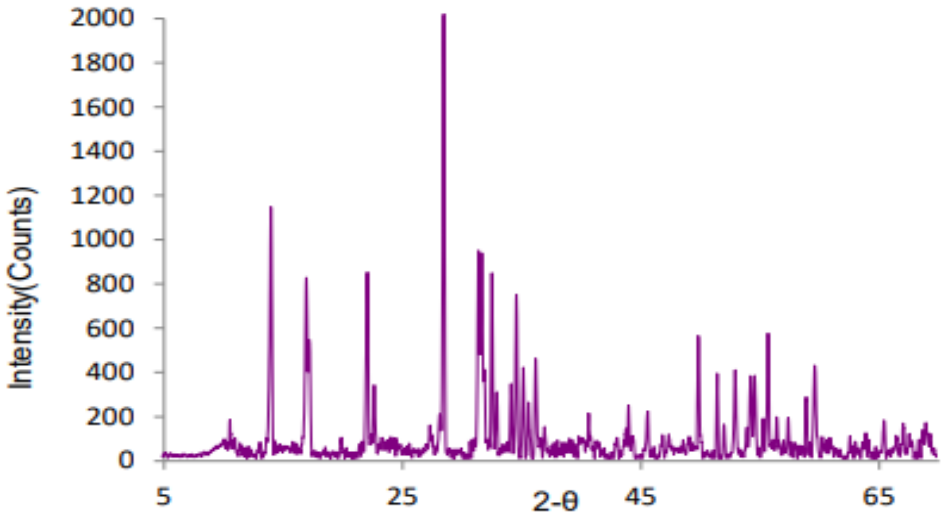

Figure S13. XRD pattern for CQ,Ibu-Cu.complex.

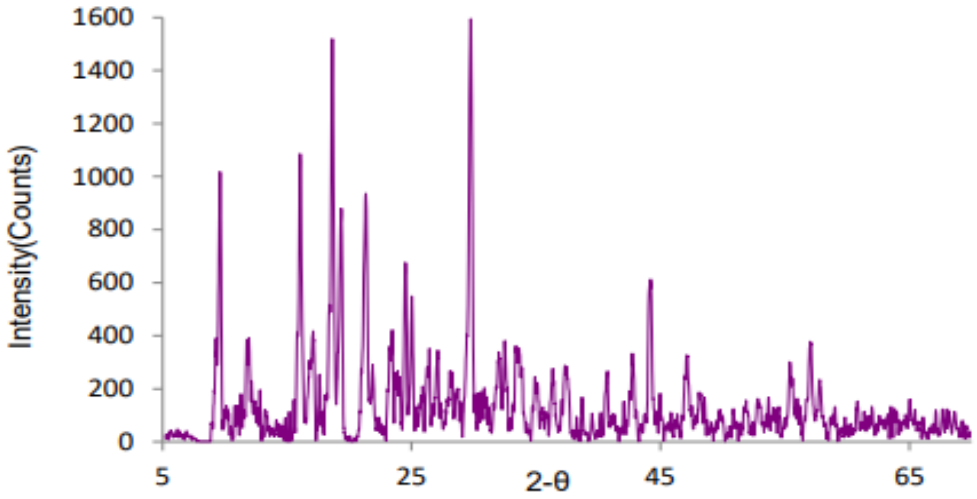

Figure S14. XRD pattern for CQ,Ibu-Zn.complex.

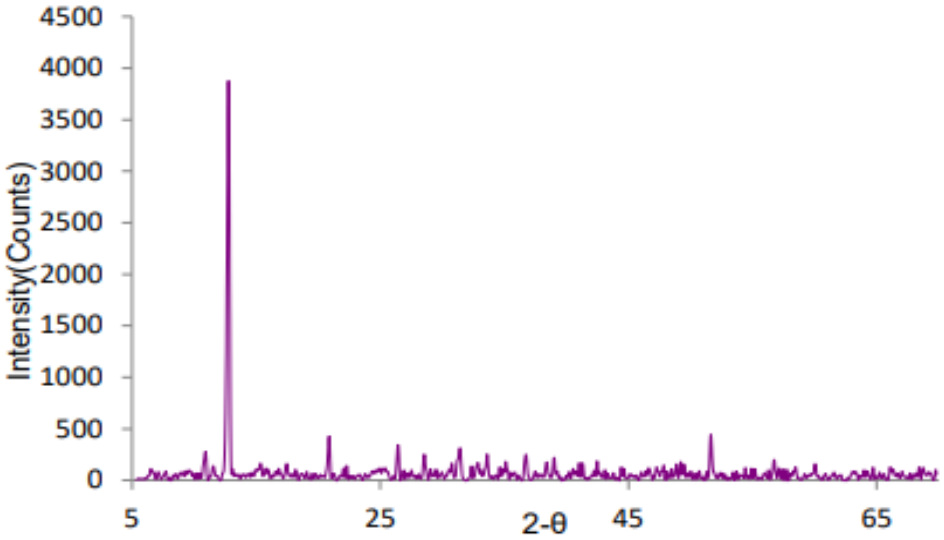

Figure S15. XRD pattern for CQ,SMX-Co complex.

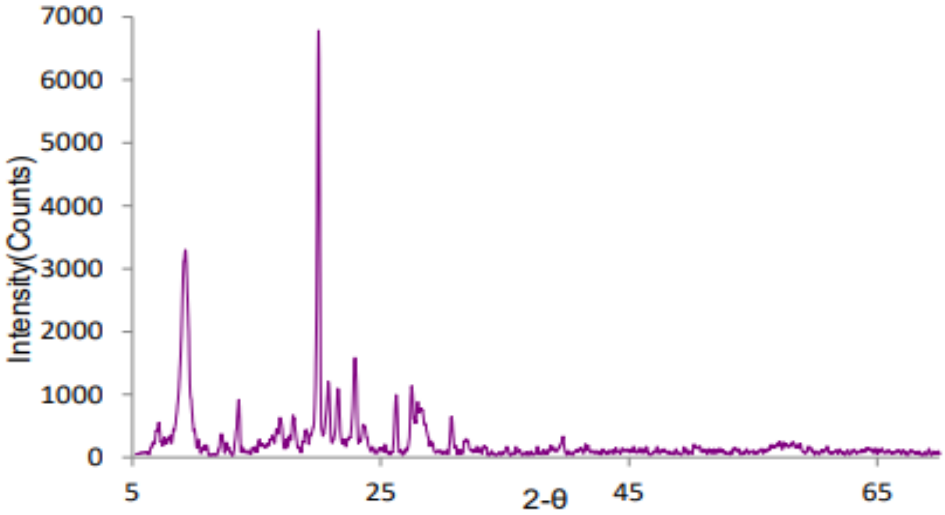

Figure S16. XRD pattern for CQ,SMX-Cu complex.

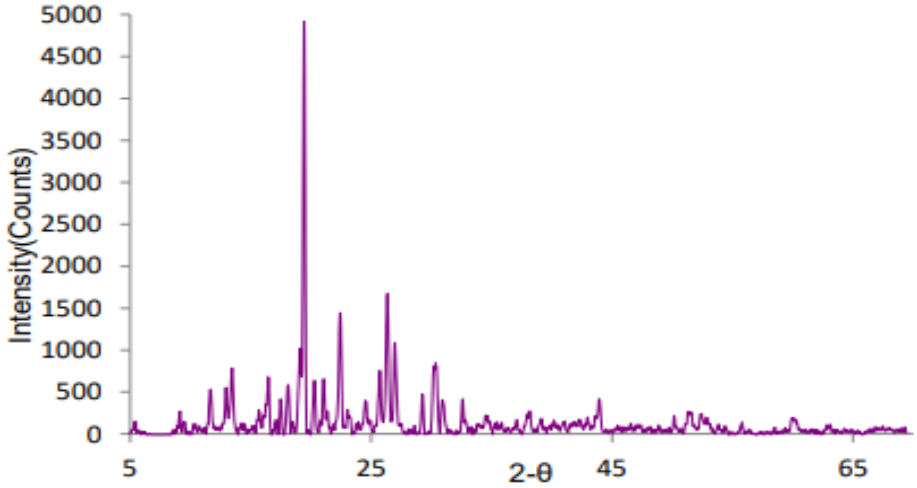

Figure S17. XRD pattern for CQ,SMX-Zn complex.

https://doi.org/10.26850/1678-4618.eq.v49.2024.e1526

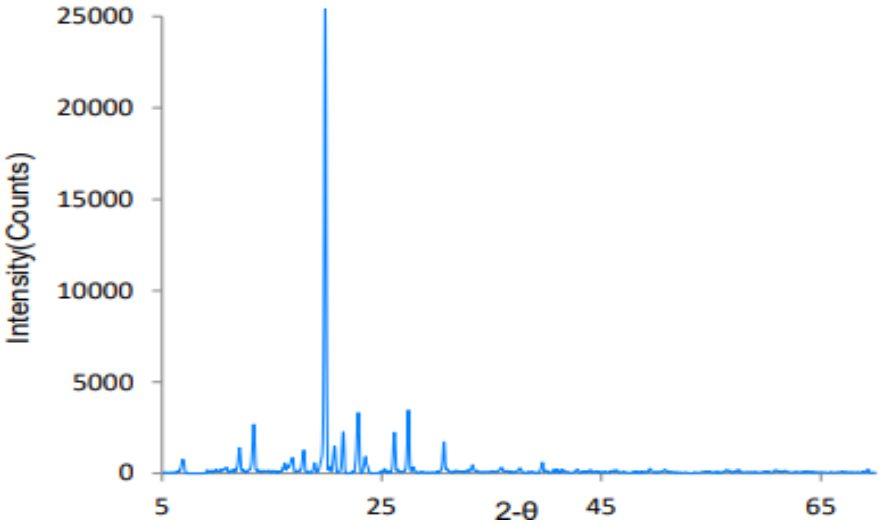

Figure S18. XRD pattern for sulphamethoxazole.

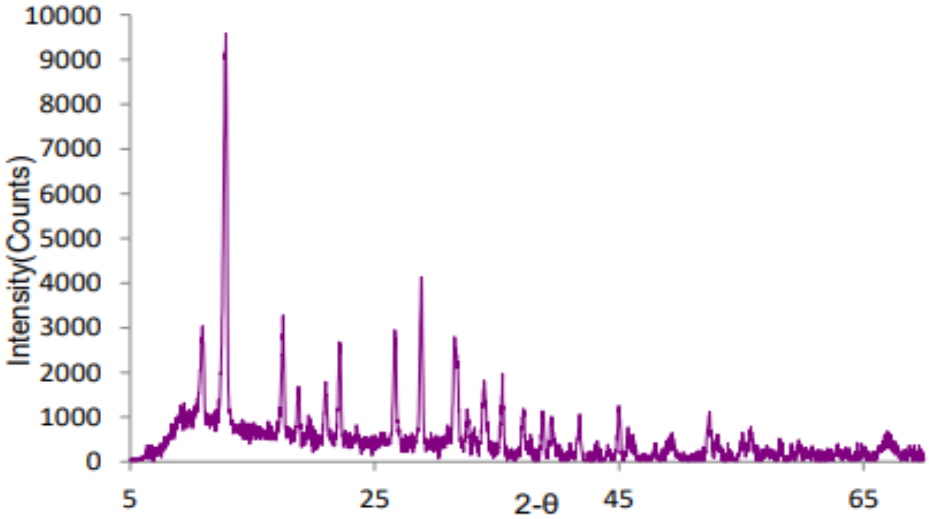

Figure S19. XRD pattern for CQ,SMX-Ni complex.

https://doi.org/10.26850/1678-4618.eq.v49.2024.e1526

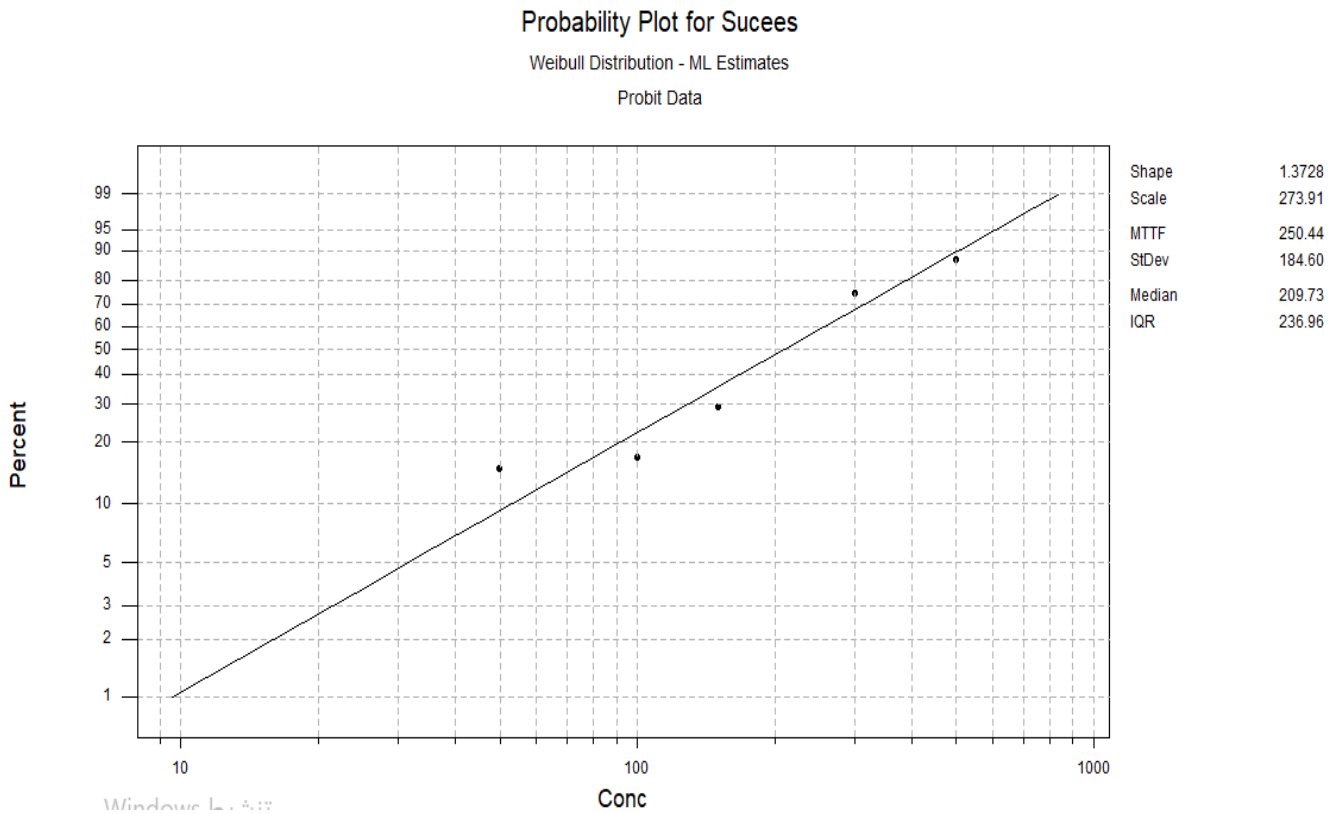

Figure S20. The relationship between concentration of CQ,Ibu-Cu complex and mortality percentage of *Ae. aegypti* larvae.

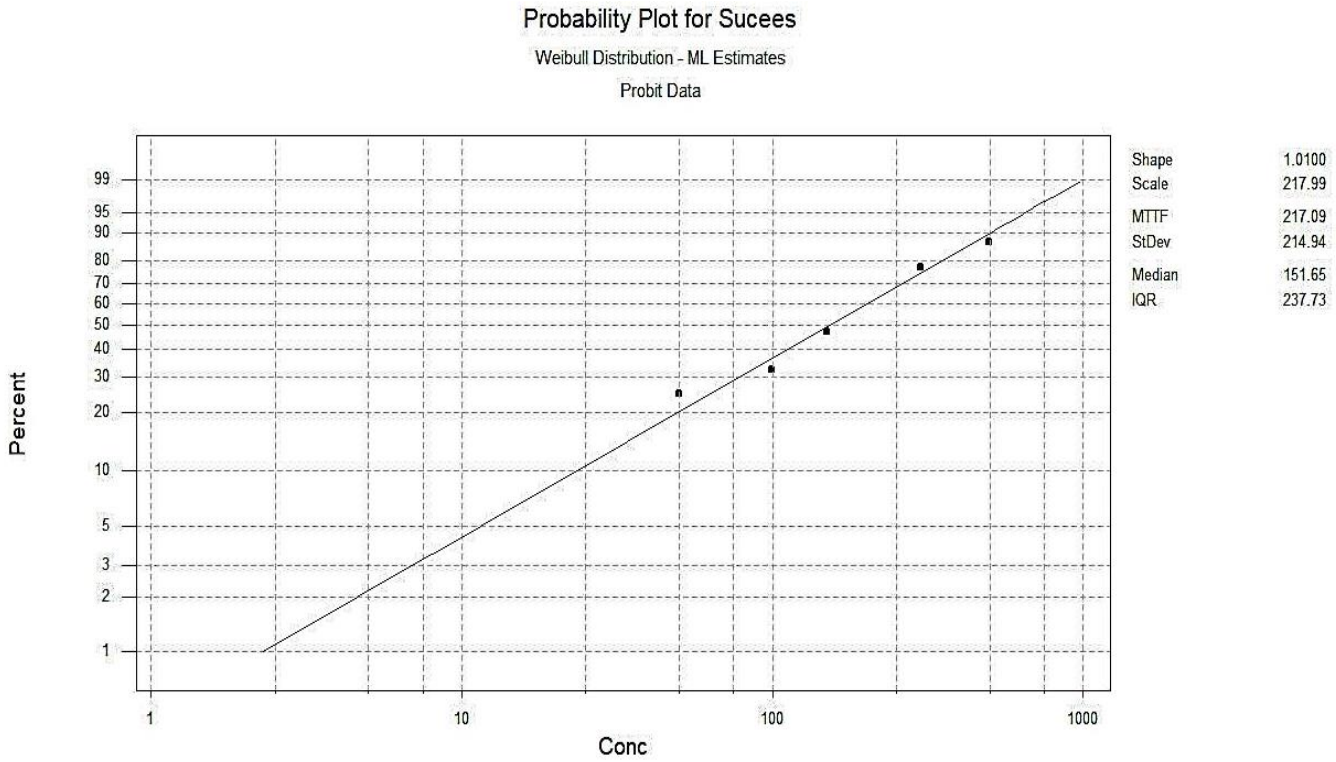

Figure S21. The relationship between concentration of CQ,SMX-Cu complex and mortality percentage of *Ae. aegypti* larvae.

Table S1. Significant IR spectral bands (cm^{-1}) of complexes with chloroquine and ibuprofen.

[Ni(CQ)(Ibu)$(H_2O)_2$Cl]	[Co(CQ)(Ibu)$(H_2O)_2$Cl]	[Cu(CQ)(Ibu)$(H_2O)_2$Cl]	[Zn(CQ)(Ibu)$(H_2O)_2$Cl]	Assignment
3215 br &w	3210 br & w	3195 br & w	3220 br & w	v(NH)
3388 br &s	3448 br & w	3467 br & w	3422 br & w	v(OH) of H_2O
1626 sh&w	1633 sh & w	1637 sh & w	1638 sh & w	Benzene ring +pyridine ring stretch
2959 sh&w	3064 sh & w	2954 sh & m	2955 sh & w	vCH–arom
2859 sh&w	2859 sh & w	2867 br & w	2853 sh & w	vCH–aliph
1101 sh&m	1102sh & m	1053 sh & m	1115 sh & m	v(C–N)
1722 sh&m	1723 sh & m	1720 sh & w	1720 sh & m	v(C=O)
1467 sh&w	1459 sh & w	1462 sh & w	1458 sh & w	v(C=N)
416 sh&w	420 sh & w	445 sh & w	419 sh & w	v(M–O)

Note: w = weak; m = medium; s = strong; br = broad; sh= short.

Table S2. Significant IR spectral bands (cm^{-1}) of complexes with chloroquine and sulfamethoxazole.

[Ni(CQ)(SMX)$(H_2O)Cl_2$]	[Co(CQ)(SMX)$(H_2O)Cl_2$]	[Cu(CQ)(SMX)Cl_3]	[Zn(CQ)(SMX)Cl_3]	Assignment
Overlab with v(OH) of H_2O	Overlab with v(OH) of H_2O	3298 sh & s	3298 sh & s	v(NH)
3440 br & m	3453 br & m	–	–	v(OH) of H_2O
1591 br & m	1578 sh & w	1596 sh & w	1502 sh & m	Benzene ring +pyridine ring stretch
3147 br & s	3187 br & s	3239 sh & s	3143 sh & m	vCH–arom
3030 br & w	3068 br & s	3066 sh & s	2958 sh & s	vCH–aliph
1076 sh & w	1068 sh & w	1091 sh & s	1091 br & w	v(C–N)
1383 sh & w	1383 sh & w	1382 sh & s	1366 sh & s	v(O=S=O)
1483 sh & w	1490 sh & w	1502 sh & w	1502 sh & w	v(C=N)
483sh & w	410sh & w	419 sh & w	421 sh & w	v(M–O)

Note: w = weak; m = medium; s = strong; br = broad; sh= short.

Table S3. XRD spectra data of the principal intensity values of the ligands chloroquine, ibuprofen, and their complexes with (Ni,Co,Cu, and Zn).

Compound	2θ	β	D (nm)	Mean D	X_C (%)
CQ.	19.581	0.223	6.5895	7.056	100
	26.259	0.231	6.4369		
	21.321	0.181	8.1409		
Ibu	12.16	0.422	3.451	3.658	100
	16.70	0.389	3.762		
	20.16	0.301	4.886		
	22.30	0.397	3.718		
	24.64	0.600	2.470		
CQ,Ibu–Ni complex	10.16	0.357	4.0725	4.422	3.201
	32.26	0.316	4.7704		
CQ,Ibu–Co complex	7.121	0.622	2.3327	2.998	4.600
	7.379	0.620	2.3405		
	7.62	0.620	2.3407		
	8.40	0.387	3.7519		
	13.101	0.345	4.2247		
CQ,Ibu–Cu complex	14.841	0.216	6.761	4.821	23.017
	18.04	0.379	3.869		
	18.30	0.422	3.476		
	30.459	0.174	8.625		
	33.60	0.331	4.569		
	33.88	0.408	3.710		
	34.101	0.553	2.739		
CQ,Ibu–Zn complex	9.780	0.364	3.9929	4.4054	24.366
	16.740	0.298	4.9119		
	19.539	0.314	4.6795		
	20.319	0.303	4.8553		
	22.440	0.408	3.6183		
	31.56	0.344	4.3744		

Table S4. XRD spectra data of the principal intensity values of the ligand's chloroquine, sulphamethoxazole and their complexes with (Ni, Co, Cu, and Zn).

Compound	2θ	β	D (nm)	Mean D	X_C (%)
CQ.	19.581	0.223	6.5895	7.056	100
	26.259	0.231	6.4369		
	21.321	0.181	8.1409		
SMX.	13.98	0.247	5.9066	6.570	100
	20.98	0.205	7.1839		
	24.22	0.253	5.8539		
	29.121	0.204	7.3339		
CQ, SMX –Ni complex	11.4	0.334	4.3571	5.058	61.386
	13.46	0.332	4.3919		
	18.5	0.216	6.7924		
	22.259	0.261	5.6545		
	28.342	0.271	5.5111		
	30.682	0.248	6.0547		
	33.602	0.403	3.7534		
	36.22	0.351	4.3408		
	37.837	0.203	7.5409		
	39.699	0.28	5.4983		
	44.484	0.895	1.7480		
CQ, SMX –Co complex	13.1	0.244	5.9737	4.789	23.513
	21.9	0.279	5.2864		
	26.34	1.111	1.3386		
	33.339	0.323	4.6798		
	55.24	0.245	6.6706		
CQ, SMX –Cu complex	9.3	0.696	2.0874	3.5754	92.978
	20.88	0.237	6.2128		
	28.98	0.341	4.3860		
	29.52	0.927	1.6154		
CQ, SMX –Zn complex	14.279	0.308	4.7382	4.9042	32.538
	20.4	0.505	2.9135		
	20.759	0.2	7.3608		
	24.00	0.274	5.4029		
	28.24	0.269	5.5509		
	28.901	0.325	4.6011		
	32.58	0.401	3.7621		

Table S5. Date mortality of larvae after 24 h for chloroquine, Ibuprofen, and their complex.

Compound	Percentage of mortality of *Aedes aegypti* after 24 h
Water	0
DMSO 3%	0
CQ1000ppm	50
Ibu 1000ppm	100
CQ,Ibu–Ni 1000ppm	50
CQ,Ibu–Co 1000ppm	0
CQ,Ibu–Cu 1000ppm	100
CQ,Ibu–Zn 1000ppm	80
CQ300ppm	20
Ibu 300 ppm	70
CQ,Ibu–Ni 300ppm	40
CQ,Ibu–Co 300ppm	0
CQ,Ibu–Cu 300ppm	70
CQ,Ibu–Zn 300ppm	20

Table S6. Date mortality of larvae after 24 h for chloroquine, sulphamethoxazole and their complex.

Compound	Percent mortality of larvae after 24 h
DMSO 3%	0
CQ1000 ppm	50
CQ300 ppm	20
SMX 1000 ppm	0
SMX 300 ppm	0
CQ,SMX–Ni 1000ppm	0
CQ,SMX–Co 1000ppm	0
CQ,SMX–Cu 1000ppm	100
CQ,SMX–Zn 1000ppm	40
CQ,SMX–Ni 300ppm	0
CQ,SMX–Co 300ppm	0
CQ,SMX–Cu 300ppm	80
CQ,SMX–Zn 300ppm	20